MERCURY PHOTOSENSITIZED REACTIONS OF FLUOROMETHANES

A Thesis Submitted for the Degree of

Master of Philosophy

in the

University of Southampton

by

John Douglas Allen

Department of Chemistry

February, 1968

ACKNOWLEDGEMENTS

The investigations described in this thesis were carried out in the Chemistry Department of the University of Southampton between October, 1966 and December, 1967.

I would like to thank my supervisor, Dr. M. C. Flowers, for the welcome advice and encouragement he offered me throughout the course of this work.

I am also indebted to my parents for their unfailing support, and to Miss A. Gale who was responsible for the typing.

Finally, grants from the Central Electricity Generating Board and Chemistry Department funds are gratefully acknowledged.

C O N T E N T S

LIST OF FIGURES

ABSTRACT

FACULTY OF SCIENCE

CHEMISTRY

Master of Philosophy

MERCURY PHOTOSENSITIZED REACTIONS OF FLUOROMETHANES

by John Douglas Allen.

The efficiency with which hydrogen quenches excited mercury $6(^3P_1)$ atoms to the ground state is very much greater than that for the fluoromethanes. Consequently for approximately 1:1 mixtures of hydrogen with fluoroform, difluoromethane or methyl fluoride, only quenching by hydrogen to yield hydrogen atoms is important. In this way, hydrogen abstraction from the fluoromethanes was studied, the final product in all three cases being almost entirely methane. The activation energy for hydrogen abstraction from fluoroform by hydrogen atoms was found to be $\geq$ 9.4 kcal.mole^{-1}. The existence of methylene intermediates, formed by the elimination of hydrogen fluoride from chemically activated fluoromethanes, is suggested, and possible reaction mechanisms are discussed.

Chemical quenching of excited mercury atoms by methyl fluoride was observed in the absence of added hydrogen, and the quenching mechanism is discussed in terms of a collision complex between mercury and methyl fluoride. The formation of products was studied as a function of time, temperature and pressure, and appeared to proceed by two

alternative routes, one of which involves methylene as an intermediate. The elimination of hydrogen fluoride from vibrationally excited products was observed, and elimination-to-stabilization rate constant ratios have been determined in the cases of $CH_3.CH_2F$ and $CH_2.CH_2F$.

C H A P T E R I

INTRODUCTION

The increasing availability of fluorine compounds since World War II has led to rapid advances in the field of fluorine chemistry. As organic fluorine compounds have become more readily available, the study of their properties has emphasised their chemical stability. The high strength of the carbon-fluorine bond, which is inert to mono - or biradical attack, has caused these compounds to be of particular interest to the gas kineticist. Among the first compounds to be studied from this point of view were 1, 1, 1-trifluoro acetone[1], trifluoroacetaldehyde[2], and hexafluoroacetone[3], which undergo photodecomposition reactions similar to their hydrocarbon analogues, producing the trifluoromethyl radical. The kinetic parameters for the hydrogen abstraction by CF_3 radicals have been determined for a number of hydrocarbons [4], [5].

Early kinetic studies of the reactions of fluorocarbons were limited to the use of optical and mass spectrometry, and chemical methods of analysis of reaction products. The comparatively recent arrival of vapour phase chromatography(v.p.c.) has not only simplified analysis but vastly improved the accuracy. Product identification and quantitative estimation at very small percentage conversions is now a simple task, previously impossible except by mass spectrometry where isotopic substitution was used.

Many chemical reactions, especially those of organic compounds proceed via a free radical mechanism. Kinetic studies require the variation of these radical concentrations, whilst keeping other

reaction parameters as constant as possible. Thermal methods of radical production are often unsuitable since the high temperatures required may cause the reaction under investigation to proceed too fast to be readily followed. The most convenient method is by photolysis, either directly as in the acetones above, or indirectly by the use of photosensitizer. The process of photosensitization involves the absorption of light by a strongly absorbing substance, the photosensitizer, and transference of the excitation energy to another compound which does not absorb, or absorbs only weakly, in the spectral region employed. The advantage of photosensitization is that light of sufficient energy to induce chemical reaction may be indirectly transferred to the compound in a region where it does not itself absorb. Some metal vapours are useful as photosensitizers in the ultraviolet spectral region. Mercury is particularly important as it possesses a high vapour pressure at low temperatures and can be irradiated with a low pressure mercury arc lamp to excite the mecury atoms to the triplet ($^3P_1$) state. If these excited atoms are quenched in a chemical process in which the $Hg(^3P_1)$ atom returns to the ground state, $Hg(^1S_o)$, the quenching molecules gain 112.2 Kcal/mole. Alternatively, the quenching proceeds by a one-step dissociation process, as appears to be the case with hydrogen and paraffins:

e.g. $Hg^* + H_2 \longrightarrow H_g + H + H$;

where Hg^* denotes the ($^3P_1$) state, and Hg denotes the ground state.

Different compounds possess different efficiencies for the

quenching process, the quenching efficiency being expressed either as the bimolecular quenching rate constant, or the effective collisional cross-section of the quencher. The primary process in the quenching of triplet mercury by saturated hydrocarbons always appears to be a C-H bond fission, and the quenching efficiencies are relatively low in many instances. With olefins and triplet mercury, formation of excited molecules in the primary quenching step predominates, and in these cases the quenching cross-sections are always very large. If a sufficiently low-lying triplet electronic state is not available and the ground state of the quenching molecule is singlet, the transfer of energy into vibrational energy of the ground electronic state of the quencher is spin-forbidden, and quenching will normally proceed by the fragmentation of the quenching molecule. If all bonds in the quenching molecule have dissociation energies higher than 112.2 Kcal/mole and there is no low-lying triplet state, as in carbon tetrafluoride, total physical quenching must occur. Since this is a spin-forbidden (i.e. highly inefficient) process, the quenching cross-section of CF_4 is very small. The presence of a C-H bond, as in fluoroform, creates the possibility of chemical quenching, although the quenching efficiency is still very small, as the C-H bond energy here is unusually high at 106.3 Kcal/mole[6]. The first C-F bond dissociation energy in fluoromethanes decreases from 129 Kcal/mole in CF_4[7] to 106 Kcal/mole in CH_3F[8]. Although the latter value is not very reliable, it would appear that methyl fluoride is the only case among the fluoromethanes where chemical

quenching could possibly lead to fission of the C-F bond, unless compound formation (i.e. HgF) occurs, which does not appear to be the case.

As indicated above, the mercury photosensitized decomposition of hydrogen is particularly interesting as a source of hydrogen atoms. If hydrogen is mixed with another compound of relatively low quenching cross-section, the abstraction reactions of the hydrogen atom can be studied with few complications. Hydrogen atoms produced in this way have been found to give no reaction with CF_4 up to 300°C[9], and agreement with this result was found at temperatures up to 400°C in this work. It was originally hoped to obtain the relative rate constants for the dimerization and cross-combination of CH_3 and CF_3 radicals, by the study of mixed $CH_4/CHF_3/H_2$ systems. However, a study of the CHF_3/H_2 system revealed that although C_2F_6 was formed, methane was the major product. This system was therefore studied in an attempt to determine the mechanism of the methane formation. The systems CH_2F_2/H_2 and CH_3F/H_2 were briefly investigated as they were expected to proceed by a similar mechanism. Methyl fluoride itself was found to quench excited mercury by a chemical process and it was this last system that was studied most fully.

The recombination of two small alkyl radicals produces initially a highly excited or "hot" molecule, which may be either collisionally stabilized or undergo unimolecular decomposition:

$$A + B \longrightarrow AB^*$$

$$AB^* + M \longrightarrow AB + M$$

$$AB^* \longrightarrow C + D$$

where the asterisk denotes a "hot" molecule, and M is any deactivating species. With ethyl and higher homologous radicals, the energy of recombination can be distributed among the various degrees of freedom of the molecule such that the combination process is pressure independent down to very low pressures. In the photolysis of fluorinated acetones it has been found that some of these activated molecules which contain fluorine readily eliminate hydrogen fluoride [10], [11], [12]. The rates of elimination from these "hot" fluoroethanes have been correlated with the decreasing number of effective oscillators in the molecules with decreasing fluorine atom content, in terms of the Rice-Ramsperger-Kassel theory of unimolecular reactions [13]. However, the rate of HF elimination will depend on all the following factors:[12]

(a) the vibrational energy content of the "hot" molecule (i.e. the strength of the C-C bond formed on radical combination and the temperature of the system),

(b) the F atom content and distribution in the molecule (Increasing F atom content increases the number of effective oscillators, but also probably decreases the activation energy for HF elimination, and α-fluorination promotes elimination relative to β-fluorination),

(c) the efficiency of the deactivating species in the system.

Hence , in the recombination of CHF_2 radicals at temperatures up to 300°C, the elimination of HF was found to be unimportant compared to the disproportionation reaction, (14)

$$CHF_2 + CHF_2 \longrightarrow :CF_2 + CH_2F_2 .$$

C H A P T E R II

Page

APPARATUS AND EXPERIMENTAL PROCEDURE

APPARATUS AND EXPERIMENTAL PROCEDURE

(a) Description of Apparatus

The gas handling system (Fig. 1) was a conventional Pyrex glass vacuum line capable of evacuation to 1×10^{-5} mm.Hg., using an Edwards single stage oil rotary backing pump and an Edwards mercury diffusion pump.

The furnace was constructed from Sindanyo asbestos board with Vermiculite expanded mica as a thermal insulator. The reaction vessel, a quartz cylinder 8 cm. long by 5 cm. diameter with plane end windows, was mounted horizontally in a Dural alloy cylinder, on which was wound an insulated winding of nichrome wire. By shunting tappings on this winding with external resistances, a temperature gradient of less than 0.5°C over the length of the reaction vessel was obtained at temperatures up to 400°C. The furnace temperature was set and controlled to $\pm$0.2°C by an A.E.I. RT3/2R temperature controller in conjuntion with a platinum resistance thermometer. The temperature in the vicinity of the reaction vessel was measured by a chromel/alumel thermocouple and a Tinsley potentiometer. However, towards the end of this work the temperature was found to be drifting by up to 1°C during a run (100 min.), although the fault was not located.

The reaction vessel was irradiated by a low pressure Hanovia mercury resonance lamp, in the form of a flat spiral, a constant voltage transformer feeding the manufacturer's supply unit. The essentially monochromatic radiation (2537 Å) was collimated by means

VACUUM LINE AND REACTION SYSTEM

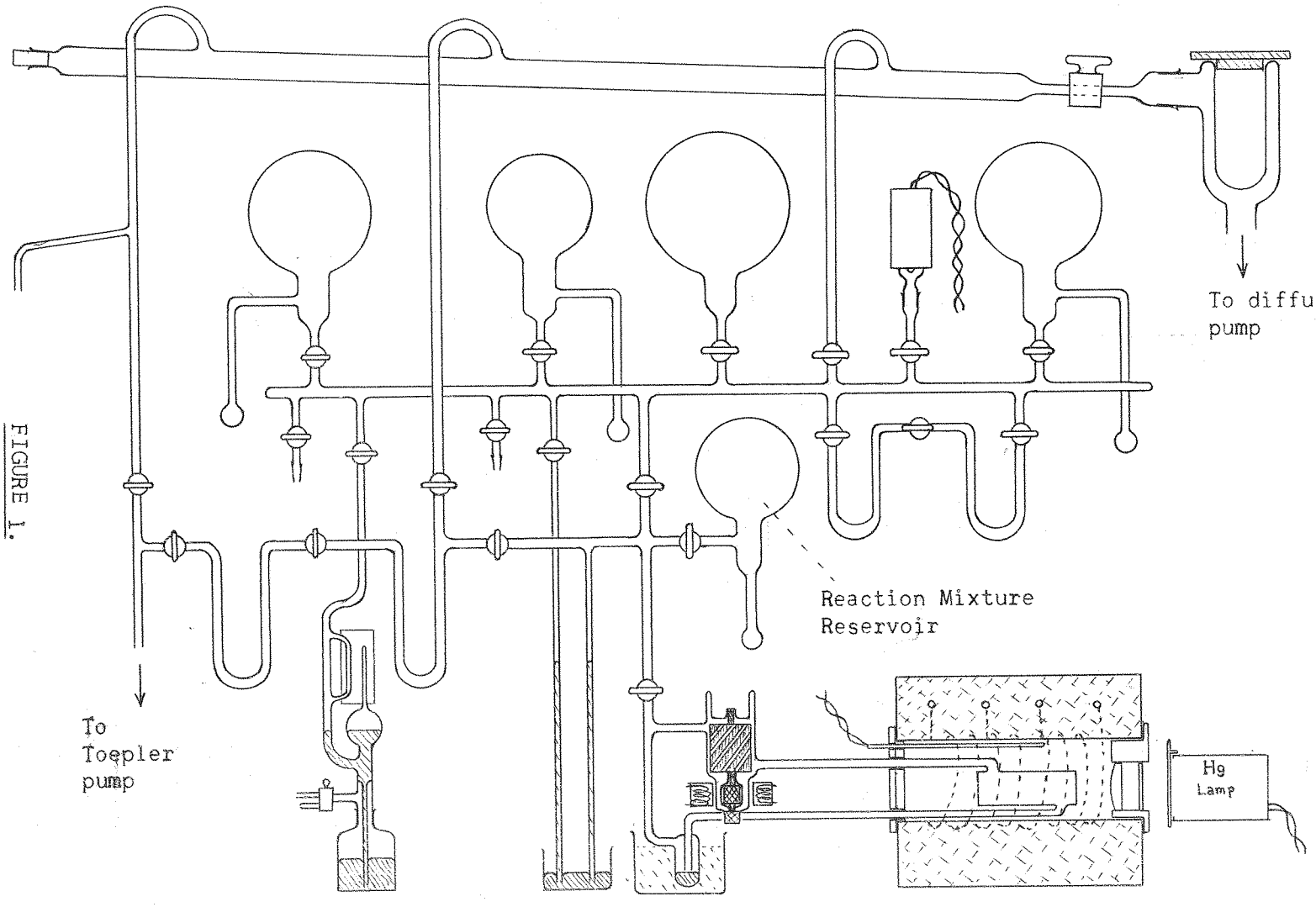

FIGURE 1.

of a 3" diameter, 3" focal length quartz lens, held in position at the end of the furnace together with a plane quartz disc.

A specially constructed teflon vane circulating pump was used to keep the reactants saturated with mercury vapour from a reservoir, held at a constant temperature of 20.0 ± 0.1°C by a thermostated water bath. The pump was driven by water cooled induction motors acting on a glass-encapsulated cylindrical copper block attached to the teflon vane and running on a teflon bearing. The pumping speed of this circulator was, however, undetermined.

The pressure of reactant gas, or gases, normally in the range 10-200 mms. Hg, was measured by a mercury manometer. Reaction products and unchanged reactant could be pumped through two cold traps in series, to separate fractions of different volatilities, by an automatic Toepler pump to a gas burette (Fig. 2). The gas could be transferred from the gas burette to sample bottles for analysis by a Perkin Elmer model 451 gas chromatograph, using a Honeywell-Brown chart recorder. The Toepler pump was specially designed to avoid the use of an internal contact, thus avoiding the possibility of decomposition of the gas being transferred by arcing at the contact (Fig. 2).

Three columns were used for analysis in the gas chromatograph, all ¼" o.d.; (a) silica gel (Perkin Elmer, type DT002), (b) alumina (one metre), and (c) PhasePak "Q", 44-60 mesh (three metres). The last two columns were made from coiled copper tubing. (PhasePak "Q" is a cross-linked polystyrene material manufactured by Phase

FIGURE 2.

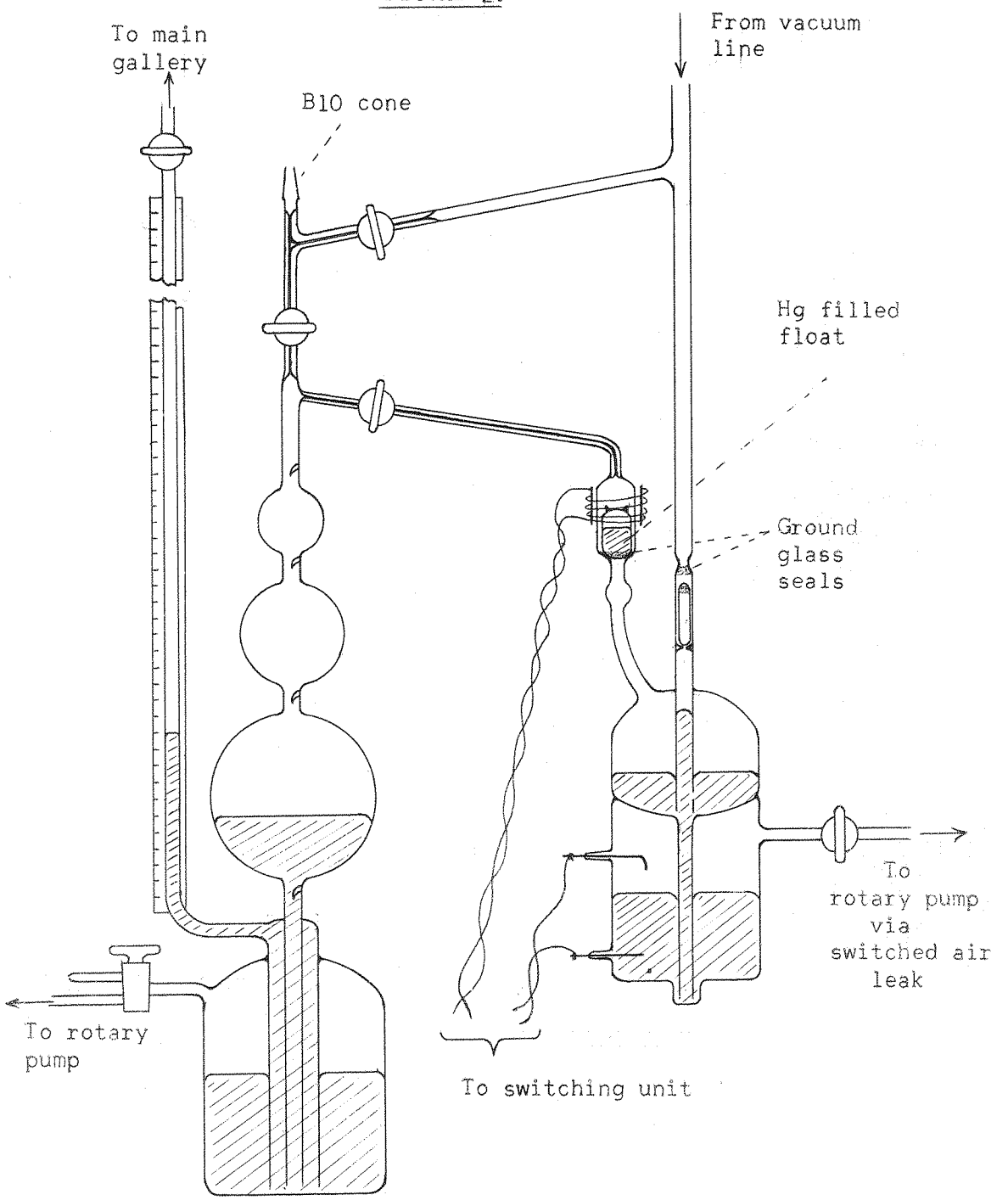

Diagram of GasBurette and Toepler Pump

Separations Ltd.) Two detectors were available for analysis, a flame-ionization detector (F.I.D.) and a hot-wire detector. The former was used almost exclusively throughout this work due to its superior sensitivity and linearity, although a pure sample of each product is required for calibration purposes as the sensitivity varies for different compounds. The hot-wire detector was used only for compounds not detected by the F.I.D., e.g. CF_4. Hydrogen was used as the carrier gas and hence no auxilliary hydrogen was required for the F.I.D. Molecular sieves were used in the hydrogen and air supply lines to remove any impurities of water and light hydrocarbons.

The gas chromatograph was fitted with a stream-splitter so that the ratio of gas flow to the parallel flame ionization and hot wire detectors could be varied by the use of different sized hypodermic needles at the flow outlet. In order to increase the sensitivity of the F.I.D. by passing all the gas to this detector, the outlet was usually blanked off by a blocked needle. In this way, several analytical runs could be made without a severe loss of sample pressure (where a low pressure of reactant was used) by retaining the small injection volume (5ccs.). The modification did, however, necessitate strict control of hydrogen flow rate and air pressure to the F.I.D., and different calibration factors for each product were found for each column, the hydrogen and air supply pressures being adjusted for maximum sensitivity.

The chart recorder was fitted with a Disc integrator which was indispensible for the measurement of the areas of early, sharp

peaks on the chromatogram. However, for peaks appearing in the tail of the reactant peak and for some of the later peaks, a planimeter, calibrated against the Disc integrator, was found to be more reliable. Using this system of analysis, concentrations in the order of one part in 10^6 of reactant could be readily obtained.

Apart from the gas chromatograph, a Metropolitan-Vickers M.S.3 Mass spectrometer and a Unicam SP200G infra-red spectrophotometer were used in the investigation of products and impurities.

(b) Experimental Procedure

The reactant gas, or mixture of gases, for a series of runs was stored in a one litre vessel connected by a tap to a small intermediate volume, fitted with a mercury manometer. This volume was connected to the mercury saturator and the reaction vessel by a single tap. The required pressure of reactants could thus be expanded into the reaction vessel by a series of expansions from the storage bulb via the intermediate volume. The total pressure in the reaction vessel was read from the manometer before the vessel and saturator were isolated. The mercury reservoir thermostat, the circulator motor and the resonance lamp were switched on at least fifteen minutes prior to a run, the lamp being isolated from the cell by a shutter during this warm-up period. The furnace temperature was found by measuring the thermocouple e.m.f. on a Tinsley potentiometer, correcting for the temperature of the cold junction and using chromel-alumel

thermocouple calibration tables. The temperature, which was checked four or five times during a run, could thus be measured to the nearest 0.1°C. When a run was started the shutter was removed from the lamp and the time noted.

At the end of a run, the shutter was replaced and usually all reactants and products transferred (via the Toepler pump) to a sample bottle, to be analysed by gas chromatography. Products were identified by the addition of pure samples of the suspected compound to the reaction mixture and comparison of the retention times. The identification was confirmed on a second column where possible. Where the concentration was high enough, the unknown product was separated from the column, by means of a trap attached to the outlet, and examined by mass spectrometry. The PhasePak "Q" column was found to be particularly useful in the separation of hydrocarbons and fluorocarbons up to C_4. Calibration factors for the F.I.D. were determined, relative to the reacting fluorinated methane, by preparing a mixture of known concentration and analysing this mixture on each column. By applying these calibration factors, product yields were obtained as molar percentages of remaining reactant.

(c) Calculation of Lamp Output

The Intensity of 2537Å radiation entering the reaction vessel, producing excited $Hg^*(^3P_1)$ atoms, can be determined by the use of

nitrous oxide as an internal actinometer. The quantum yield of nitrogen produced in the mercury photosensitized decomposition of nitrous oxide may be taken to be unity.[15] If sufficient alkane or alkene (other than methane) is added to remove all oxygen atoms produced in the reaction,

$$Hg^* + N_2O \longrightarrow Hg + N_2 + O,$$

nitrogen is the only volatile product at liquid nitrogen temperatures.

Nitrous oxide containing 2 - 3% ethylene was thoroughly degassed and irradiated in the reaction vessel for about thirty minutes. The products were then pumped through a series of two liquid nitrogen traps by the Toepler pump to the gas burette, and the number of moles of nitrogen produced calculated. The value of the incident light intensity calculated in this way was $(2.0 \pm 0.5) \times 10^{16}$ quanta/sec. A previous determination of the output of the same lamp some time before this work was started was $(3.8 \pm 0.6) \times 10^{16}$ quanta/sec. This difference was probably due to ageing of the resonance lamp, since very little formation of a deposit on the cell window was observed throughout this work.

(d) Preparation of Materials

The following gases were supplied in cylinders:

Fluoroform, vinyl fluoride, 1, 1-difluoroethane, 1, 1-difluoroethylene, propylene, hexafluoroethane, and deuterium (98%) from the Matheson Company; difluoromethane from Columbia Organic Chemicals Company; and hydrogen, methane, ethane, and ethylene from the

British Oxygen Company.

Samples of propane, n-butane and iso-butane were obtained from the Department of Scientific and Industrial Research as mass spectroscopic standards.

The fluorides C_2H_5F, $CH_2F.CH_2F$, $n\text{-}C_3H_7F$, $iso\text{-}C_3H_7F$, $n\text{-}C_4H_9F$, and $sec\text{-}C_4H_9F$ were prepared by the following method [16]. The alkyl p-toluene sulphonate was formed by adding the appropriate alcohol to p-toluene sulphonyl chloride in pyridine. The tosylate was then heated with anhydrous potassium fluoride in digol. The alkyl fluoride evolved under reduced pressure was collected in a solid CO_2/acetone trap.

Methyl fluoride was prepared by a similar method, using commercially available (B.D.H.) methyl p-toluene sulphonate. In this case no solvent was used [16], the mixture being heated to about 200°C at a pressure of 160 mm.Hg. The product was collected in a liquid nitrogen trap. The purification of methyl fluoride was carried out by gas chromatography (see Chapter 3).

Tetrafluoroethylene was prepared by thermal depolymerization of teflon, and the catalysed hydrogenation of tetrafluoroethylene over platinized asbestos was used to prepare $CHF_2.CHF_2$.

Hydrogen used in kinetic runs was purified by passage through a silver/palladium thimble at 250°C. Most other gases were purified by trap-to-trap distillations, retaining the middle fraction.

1,1,1-trifluoroethane was gratefully received as a gift from Dr. E. Whittle.

C H A P T E R III

Page

RESULTS

RESULTS

(a) Fluoroform/Hydrogen System

Known pressures of fluoroform and hydrogen (in the ratio 0.77:1.00, respectively) were allowed to mix thoroughly by thermal diffusion in the reaction mixture storage bulb before use. Kinetic runs were then carried out, at a constant pressure of 50.0 ± 0.2 mms. Hg., for irradiation times up to 200 minutes and from room temperature up to 200°C. Methane was by far the major product. Only the silica gel and alumina columns were available for analysis at this time and other products identified using these columns were, C_2H_6, CF_3CH_3, CH_2F_2 and CH_3F. Five minor unidentified products eluted from the alumina column and one other from the silica gel column. The variation of yields with time are shown in Figs. 3 - 7, for four different temperatures, and the change in yield of methane with temperature for runs of 100 minutes is shown in Fig. 8. The peak identified as ethane may be in fact due partly to hexafluoroethane although the F.I.D. has an extremely low sensitivity for this compound.

FIGURE 3.

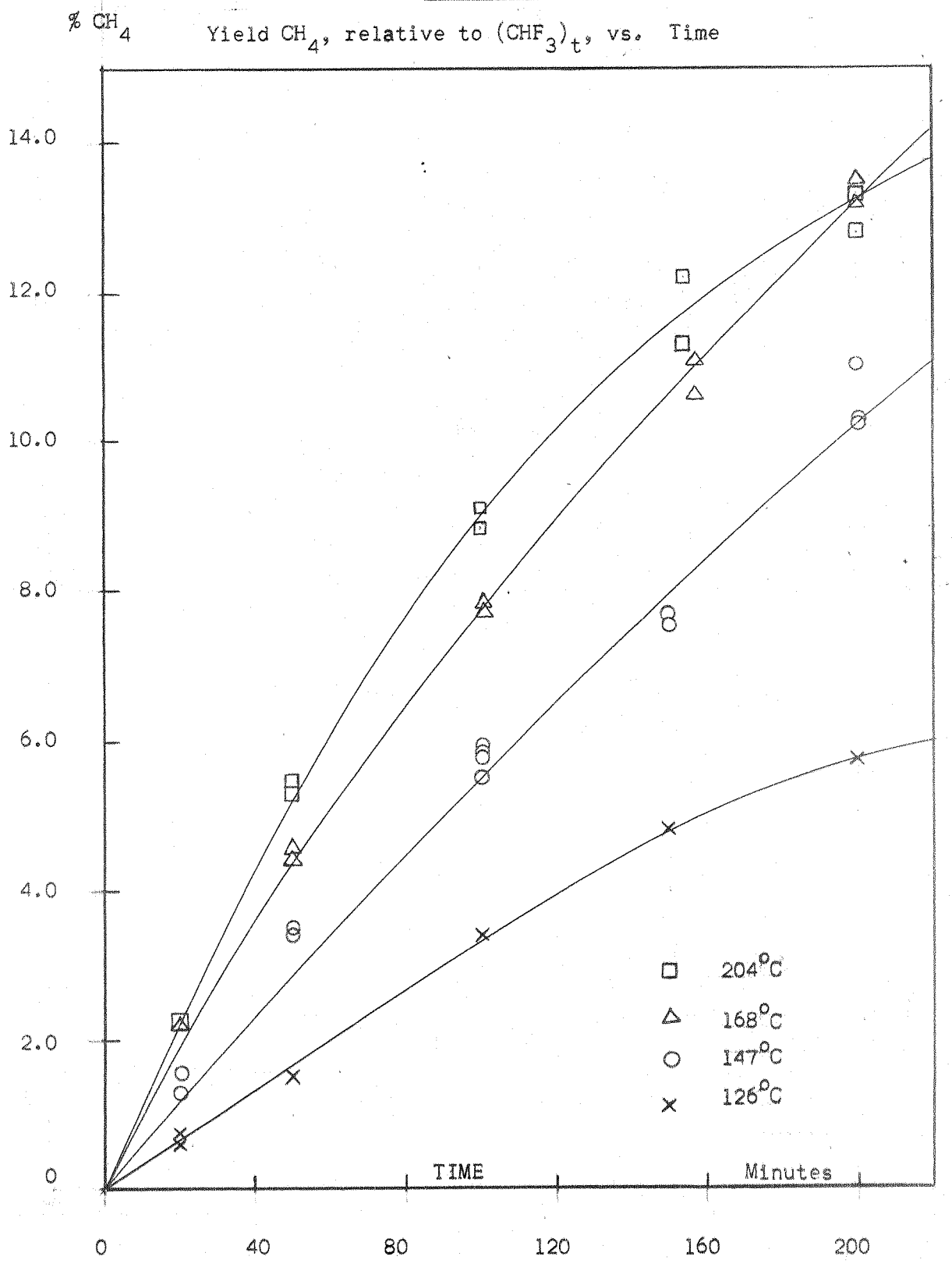
% CH_4
Yield CH_4, relative to $(CHF_3)_t$, vs. Time
14.0
12.0
10.0
8.0
6.0
4.0
2.0
0
TIME
Minutes
0
40
80
120
160
200
204°C
168°C
147°C
126°C

FIGURE 4.

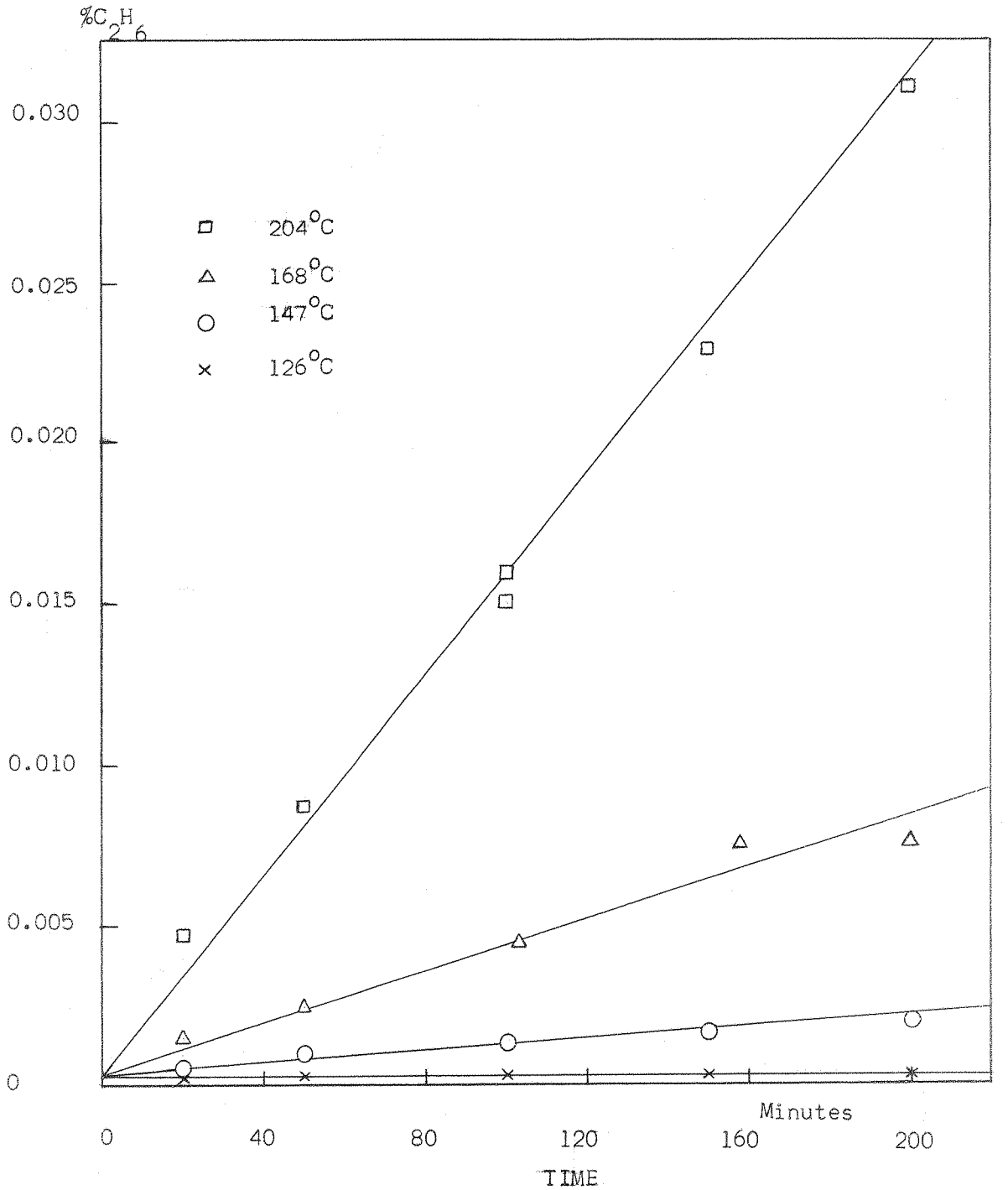

Yield C_2H_6, relative to $(CHF_3)_t$, vs. Time

FIGURE 5.

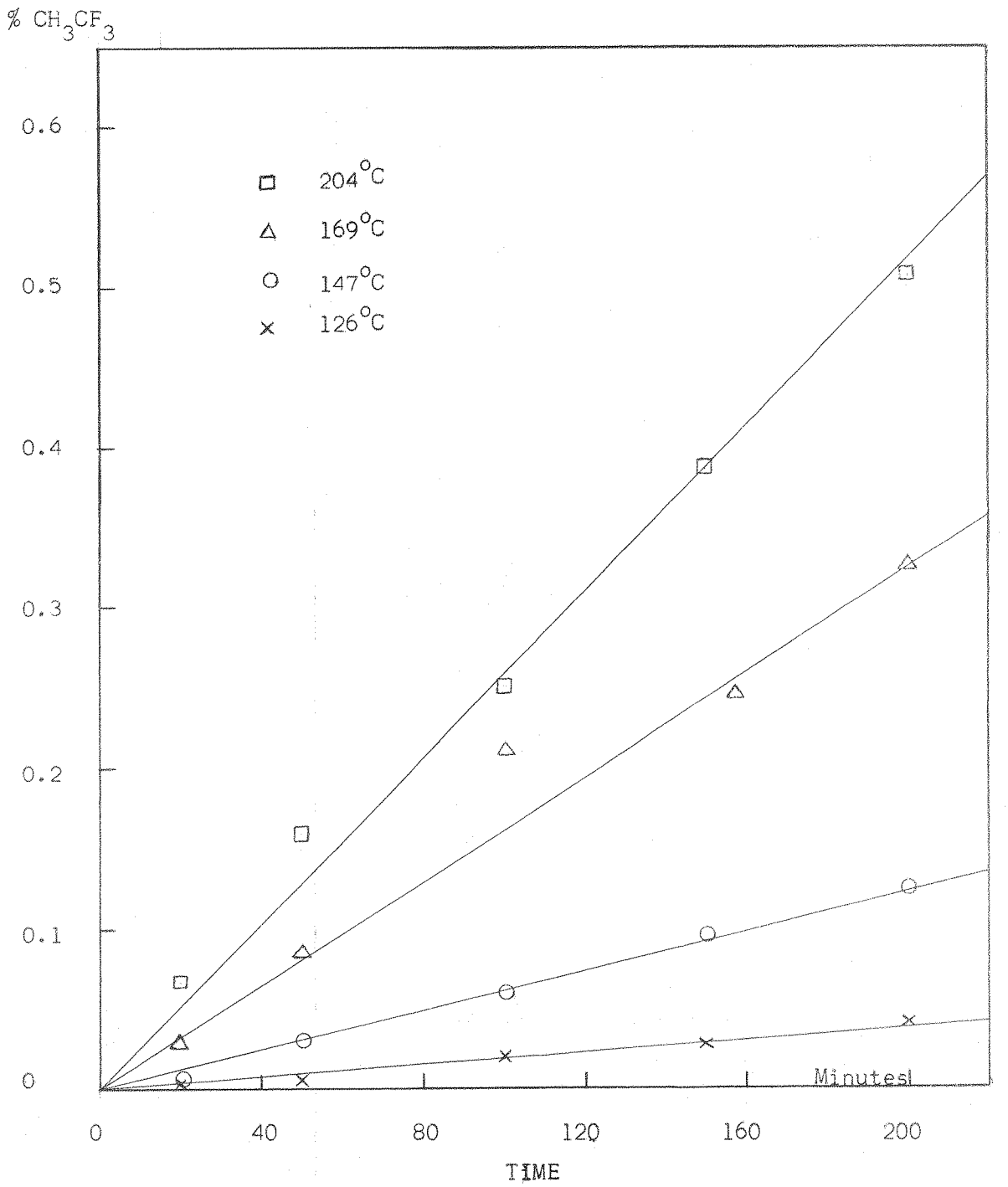

Yield CH_3CF_3, relative to $(CHF_3)_t$, vs. Time

FIGURE 6.

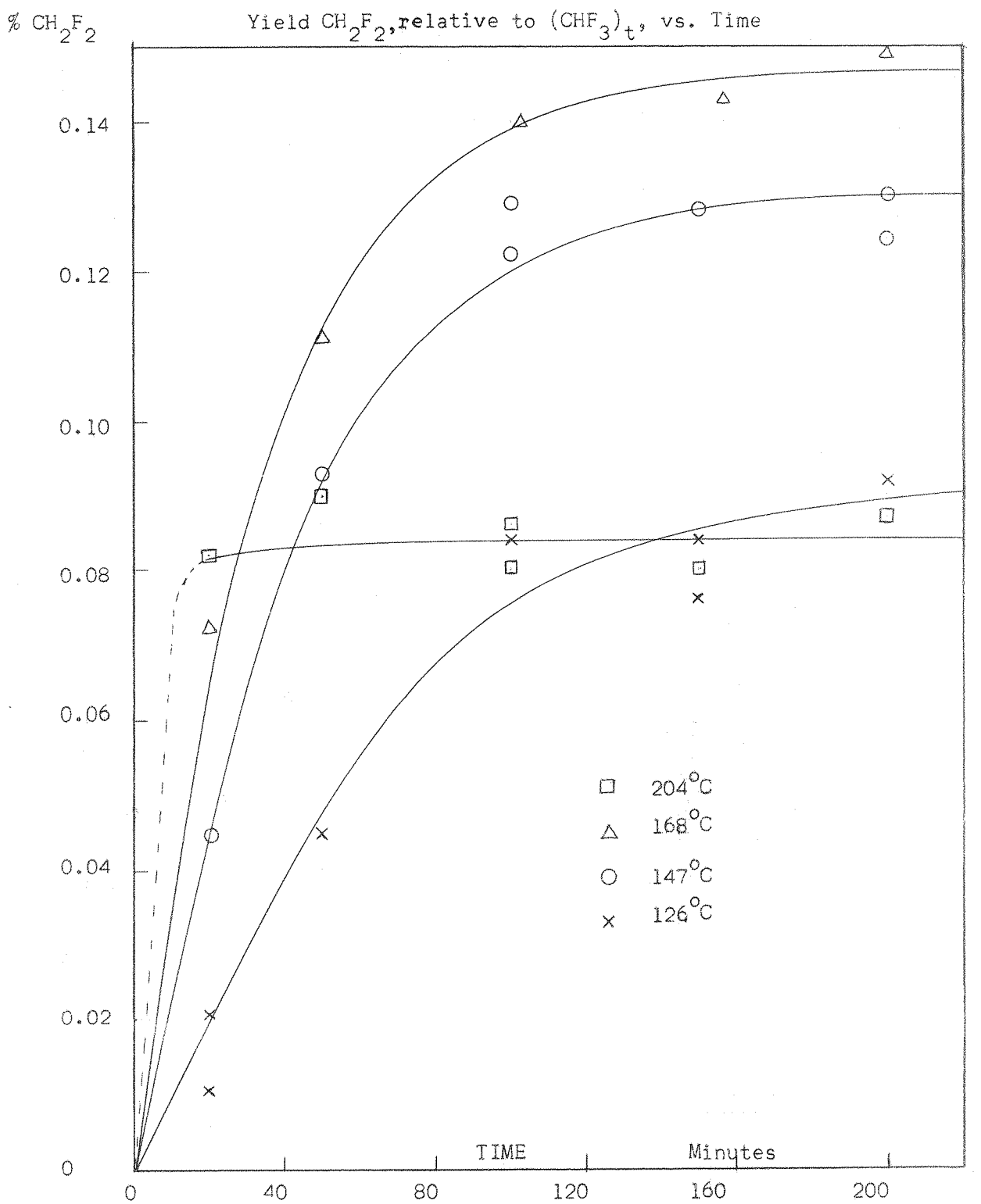
% CH_2F_2
Yield CH_2F_2, relative to $(CHF_3)_t$, vs. Time
0.14
0.12
0.10
0.08
0.06
0.04
0.02
0
204°C
168°C
147°C
126°C
TIME
Minutes
0
40
80
120
160
200

FIGURE 7

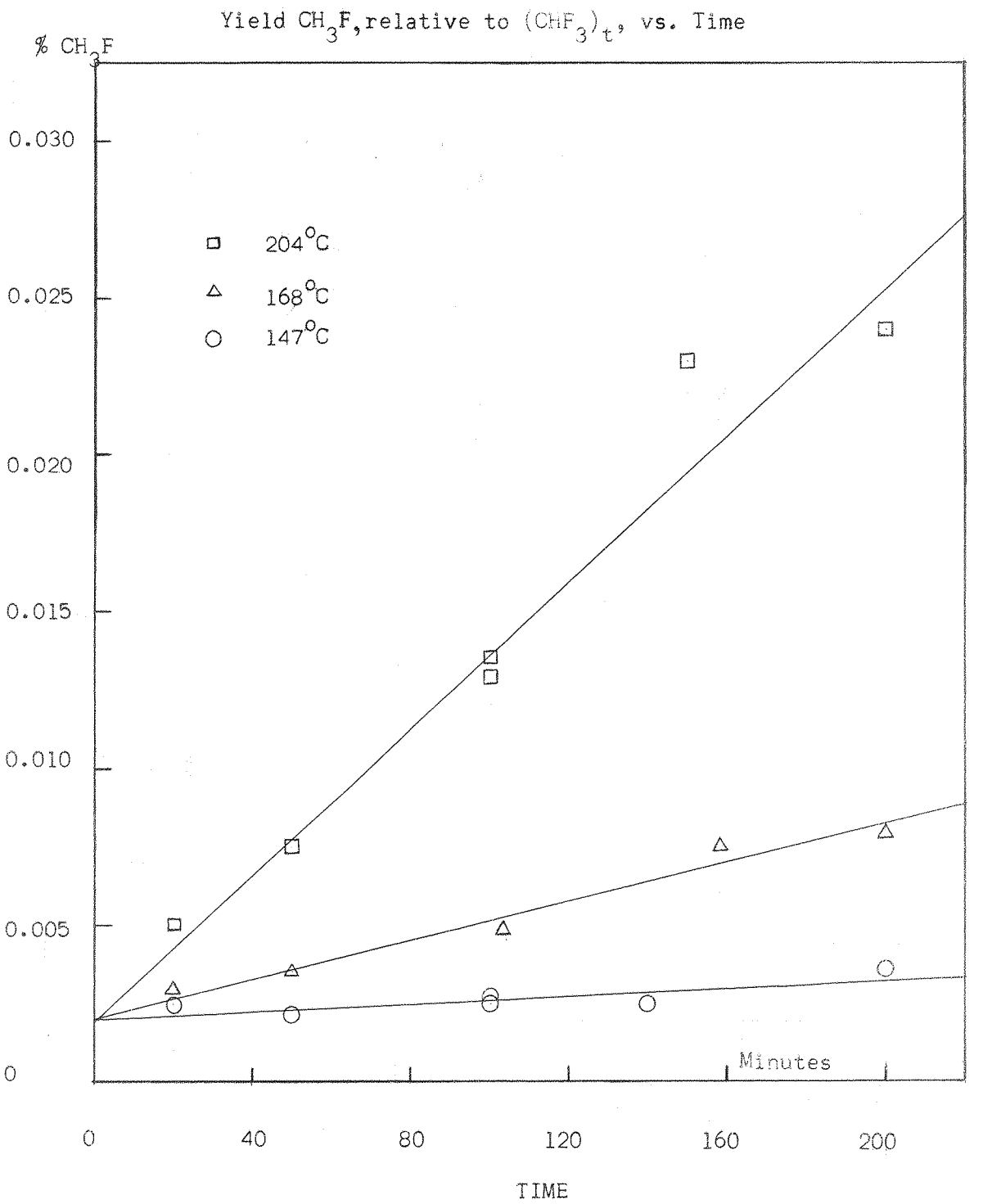
Yield CH_3F, relative to $(CHF_3)_t$, vs. Time
% CH_3F
0.030
0.025
0.020
0.015
0.010
0.005
0
204°C
168°C
147°C
Minutes
0
40
80
120
160
200
TIME

FIGURE 8

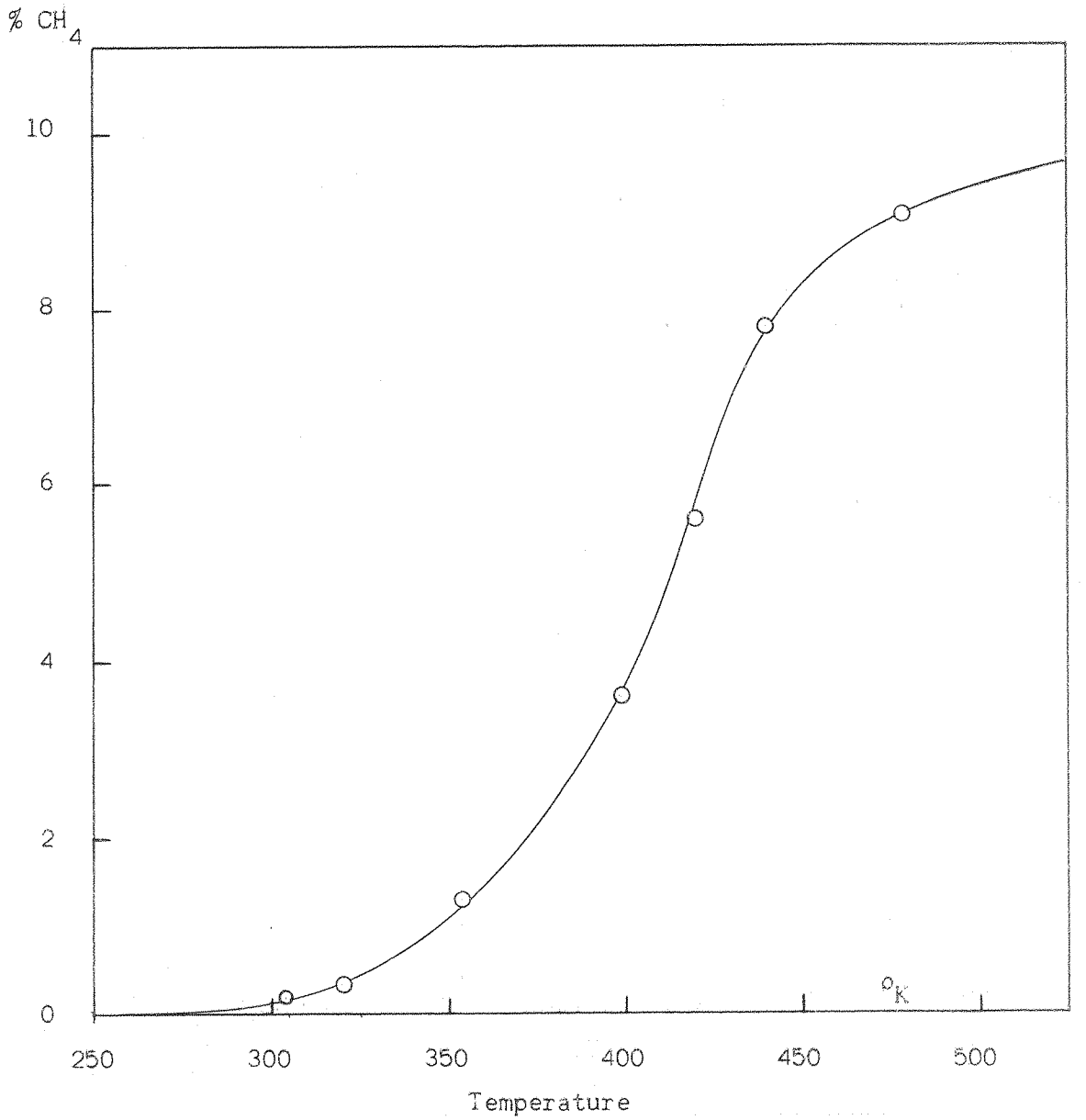

Yield CH_4, relative to $(CHF_3)_t$, vs. Temperature

Investigation of the products by mass spectrography showed a large peak at mass 85 due to the SiF_3^+ ion from SiF_4. This is formed by the reaction of hydrogen fluoride with the reaction vessel walls:

$$4HF + SiO_2 \longrightarrow SiF_4 + 2H_2O.$$

SiF_4 was also identified in the infra-red spectrum of the reaction products, as a medium strength band at about 1030cm.$^{-1}$, showing R and P branches (17).

Trifluoromethyl radicals and hydrogen atoms are obviously abundant in this system, and on recombination they form a chemically activated molecule. This activated molecule might undergo collisional deactivation or decomposition to yield difluoromethylene (c.f. reference 18):

$$CF_3 + H \longrightarrow CHF_3^* \qquad (1)$$

$$CHF_3^* + M \longrightarrow CHF_3 + M \qquad (2)$$

$$CHF_3^* \longrightarrow :CF_2 + HF \qquad (3)$$

The importance of reaction (2) was investigated by photosensitizing a CHF_3/D_2 mixture. The products of these runs where separated in two fractions, condensibles and non-condensibles at -196°C. No evidence of CDF_3 could be found by mass spectroscopic analysis, even when nearly an atmosphere of argon was added to the reactants. Therefore, reaction (3) must be much faster than (2). The increase in the proportion of DH in the deuterium also appeared to correspond to the amount of methane (CD_4) formed.

In view of the reported stability of difluoromethylene relative to methylene [19] and its unreactive nature with respect to hydrogen addition in the gas phase, [19a,d] attempts were made to produce difluoromethylene, by other means, in the presence of hydrogen and to examine for the presence of difluoromethane and methane. Sodium chlorodifluoroacetate was prepared from the acid and heated for 20 hours at 180°C. in an atmosphere of hydrogen. (This method of preparation of $:CF_2$ is well known in solution [20]. Although tetrafluoroethylene was identified in the products by gas chromatography, the major products were not identified. Difluoromethane appeared to be a minor product, and no methane was detected.

The mercury photosensitized decomposition of tetrafluoroethylene produces difluormethylene, which can then add to the double-bond to form perfluoro-cyclopropane [21]:

$$C_2F_4 + Hg^* \longrightarrow C_2F_4^* + Hg$$

$$C_2F_4^* \longrightarrow :CF_2 + :CF_2$$

$$:CF_2 + C_2F_4 \longrightarrow c\text{-}C_3F_6$$

When a little hydrogen was added to this system no methane was detected in the products and the major product, although not positively identified, was assumed to be the perfluoro-cyclopropane. With a much larger proportion of hydrogen, $CHF_2.CHF_2$ was found to be the major product. The yields of cyclo-C_3H_6 and CH_2F_2 were small but methane and ethane were identified. However, the presence

of methane and ethane does not necessarily indicate the occurrence of hydrogen atom addition to difluoromethylene. (See Discussion, section (a)).

(b) CH_2F_2/H_2 System

In view of the results obtained for the fluoroform system, similar experiments were carried out using a CH_2F_2/H_2 mixture. As expected, methane was the major product identified. Analysis was limited by the use of only the silica gel column and consequently likely products, such as CHF_2CHF_2 and CH_3CHF_2, were not identified due to their long retention time on this column. Ethane was again detected, in larger yields than in the fluoroform work, and two other product peaks were tentatively identified as propane and n-butane. Unfortunately, any methyl fluoride was lost in the tail of the difluoromethane peak.

The variation of yield of methane with time at 126°C (Fig. 9) shows a fall-off in rate of formation above a yield of about 10%, similarly to that shown in the CHF_3/H_2 runs. The rate of reaction is also shown to be faster than with fluoroform, although the hydrogen/fluoromethane ratio was higher (1.00:0.55) in this case. All runs were carried out at a total pressure of reactants of 50 mms. Hg.

(c) CH_3F/H_2 System

The photosensitized reaction of hydrogen with methyl fluoride was only briefly investigated. Preliminary runs showed that, as

FIGURE 9.

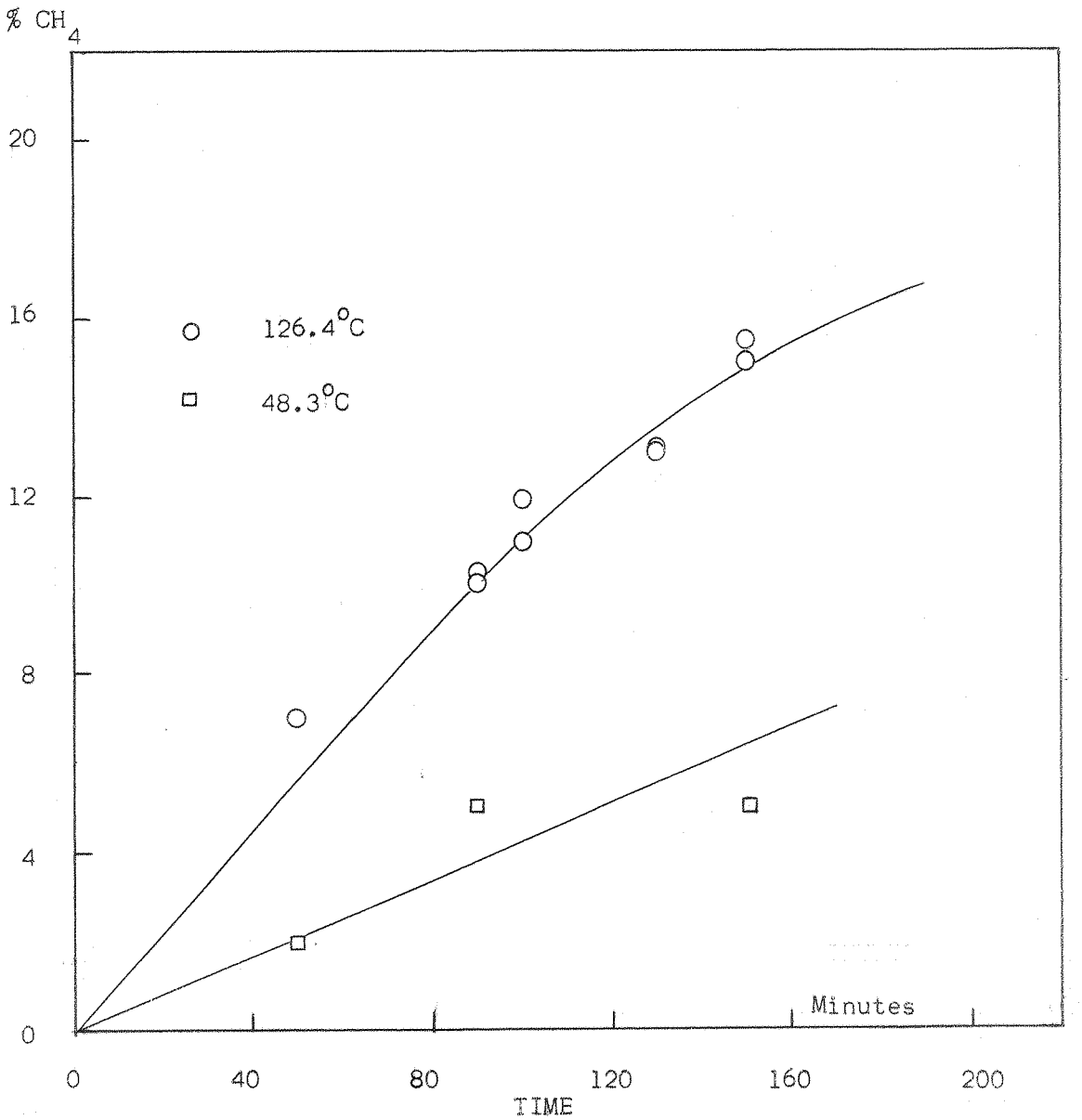

Yield CH_4, relative to $(CH_2F_2)_t$, vs. Time

before, methane and ethane were the major products. Near room temperature, methane, ethane and propane were the only products detected using the silica gel and alumina columns. At a higher temperature ($160^{\circ}C$), the methane yield appeared to be lower and several other products were separated by the alumina column, of which ethyl fluoride was identified. A later run, using purified methyl fluoride (see (d) below) and analysing the products on the PhasePak "Q" column, showed that, apart from those products mentioned, others included $CH_2F.CH_2F$, iso - C_3H_7F, n-C_3H_7F, iso - C_4H_{10}, and n - C_4H_{10}.

(d) CH_3F Alone.

Investigation of the possibility of quenching of excited ($^3P_1$) mercury atoms by fluoroform and difluoromethane yielded no evidence of reaction, although the difficulties of analysis for small yield of high-boiling, highly fluorinated products could account for this. However, under the same conditions, quenching by methyl fluoride was observed. Initial runs were analysed on the alumina column, methane, ethane, and ethyl fluoride being identified among the products.

Analysis of the methyl fluoride on alumina and silica gel columns had shown only ethyl fluoride and ethylene as very small impurities. However, after several runs had been analysed on the PhasePak column, it became evident that one of the "products"

was in fact an impurity, and examination of the starting material on this column showed it to contain about 1% of the impurity. Since trap-to-trap distillation was not effective in removing this impurity, the methyl fluoride was purified by preparative gas chromatography, using the PhasePak column. The flame ionisation detector of the Perkin Elmer "451" was isolated from the gas stream, and a trap, with inlet and outlet taps, attached to the column outlet port of the instrument. A hypodermic needle was attached to the trap outlet in order to minimise back diffusion of air into the trap (cooled in liquid nitrogen), but large enough not to restrict the flow of carrier gas (hydrogen). The hot wire detector was used to detect the effluent gases and since the separation was good, about six gas sample injections could be made in rapid succession, all the methyl fluoride being collected before the first of the impurity eluted. The trap was then transferred to the vacuum line and while still cooled in liquid nitrogen, the hydrogen pumped off. Any carbon dioxide and water were then removed by trap-to-trap distillation and the purified sample transferred to the storage vessel. By this method, the overall recovery of pure methyl fluoride was little better than 50%, but the total impurity level was reduced to about 5 parts in 10^5. The impurities remaining were propane, ethylene and ethyl fluoride.

Compared to the impure methyl fluoride, runs carried out with the purified compound showed approximately a tenfold decrease in rate of methane formation. Although several attempts were made to separate

a sample of the impurity for mass spectroscopic study, no identification could be made.

The variation of product concentrations with time (at a pressure of 50 mms.Hg.) was studied at three temperatures, 43°, 55°, and 75°C, Figs. 10 - 17). The effect of varying pressure of reactant was also studied, Figs. 18 - 23, at constant temperature (75°C) and irradiation time (100 minutes). The major products were CH_4, C_2H_6, $CH_2F.CH_2F$, and n - C_3H_7F. Other products identified were C_2H_4, C_2H_5F, C_3H_6, C_3H_8, iso - C_3H_7F, n - C_4H_{10}, and iso - C_4H_{10}. Two other products were observed, and although they were not identified, it was concluded (see Discussion, (d)) that they are likely to be $CH_3.CHF.CH_2F$ and $(CH_3)_2$ $CH.CH_2F$. The total decomposition of methyl fluoride in all runs was less than one per cent.

FIGURE 10

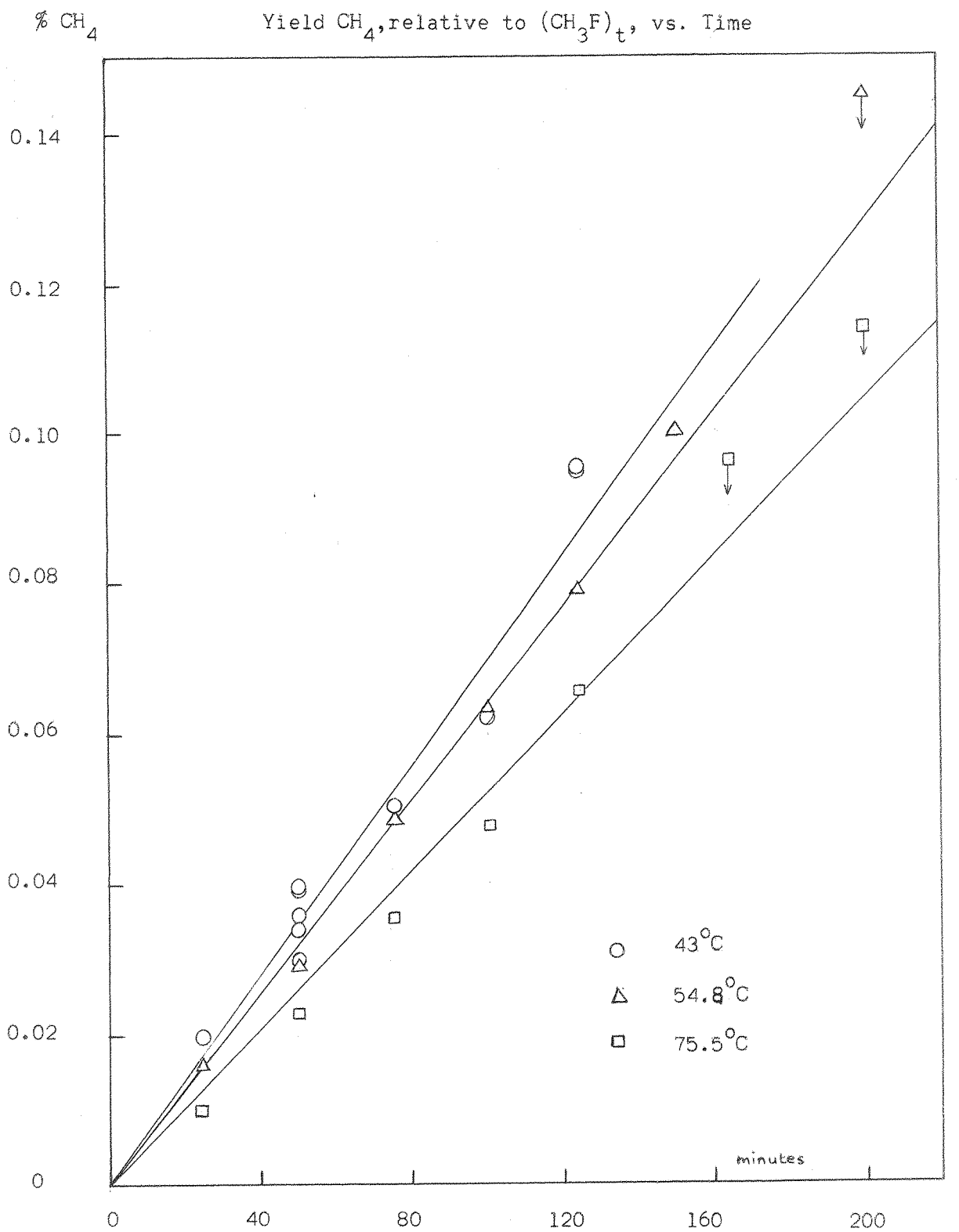
% CH_4
Yield CH_4, relative to $(CH_3F)_t$, vs. Time
0.14
0.12
0.10
0.08
0.06
0.04
0.02
0
0
40
80
120
160
200
minutes
43°C
54.8°C
75.5°C

FIGURE 11

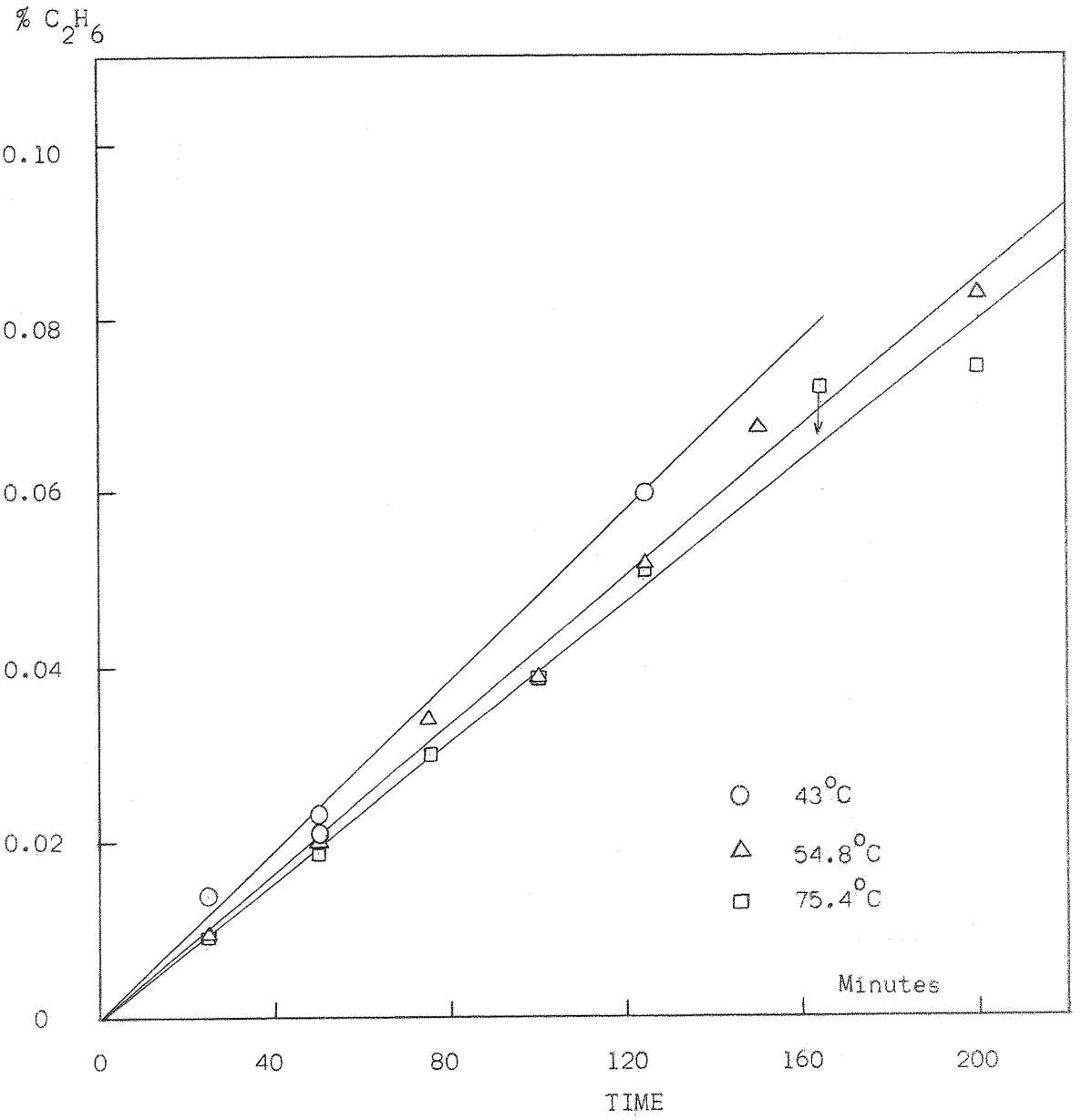

Yield C_2H_6, relative to $(CH_3F)_t$, vs. Time

FIGURE 12.

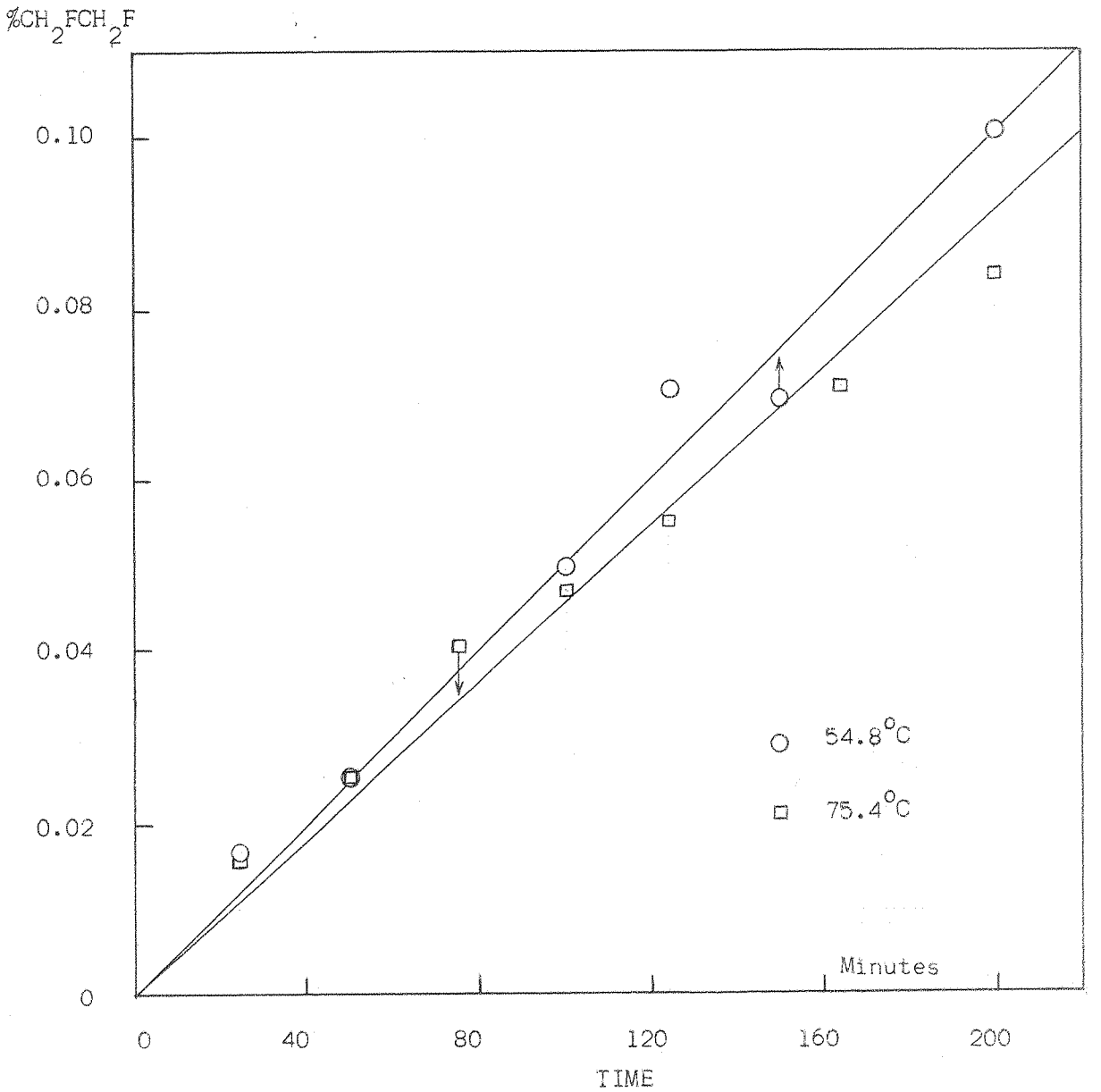

Yield $CH_2F\ CH_2F$, relative to $(CH_3F)_t$, vs. Time

FIGURE 13

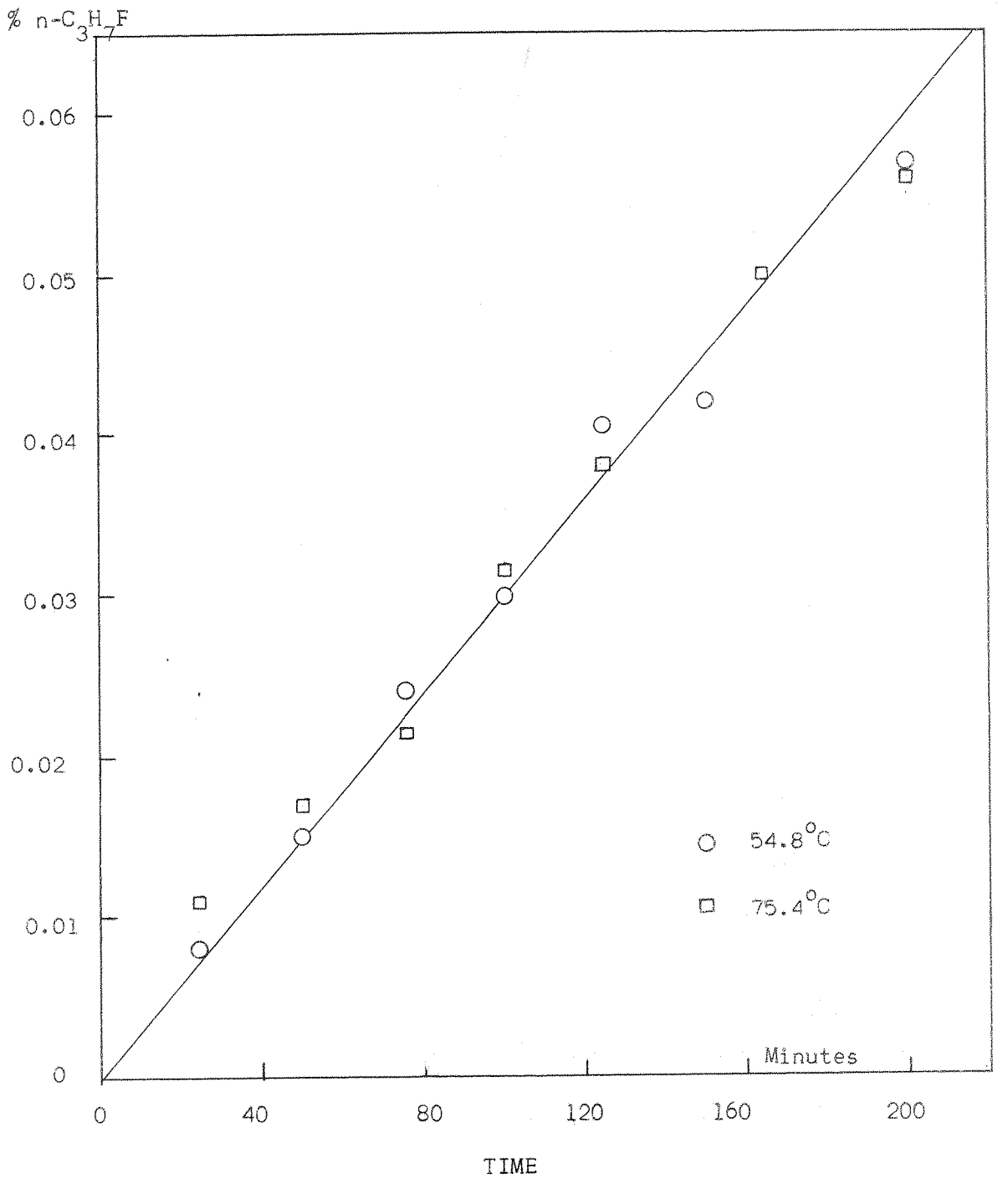

Yield $n\text{-}C_3H_7F$, relative to $(CH_3F)_t$, vs. Time

FIGURE 14.

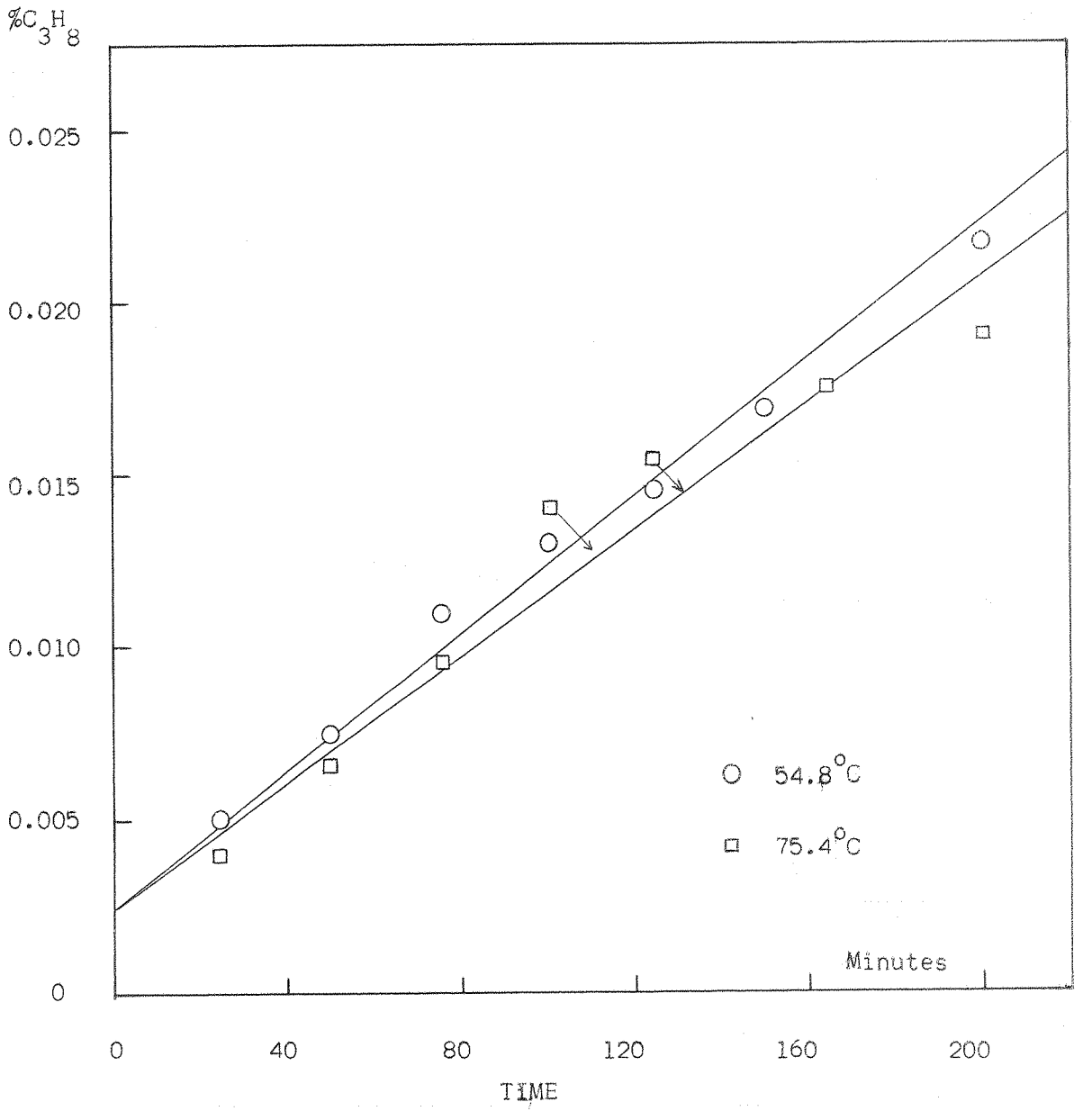

Yield C_3H_8, realtive to $(CH_3F)_t$, vs. Time.

FIGURE 15.

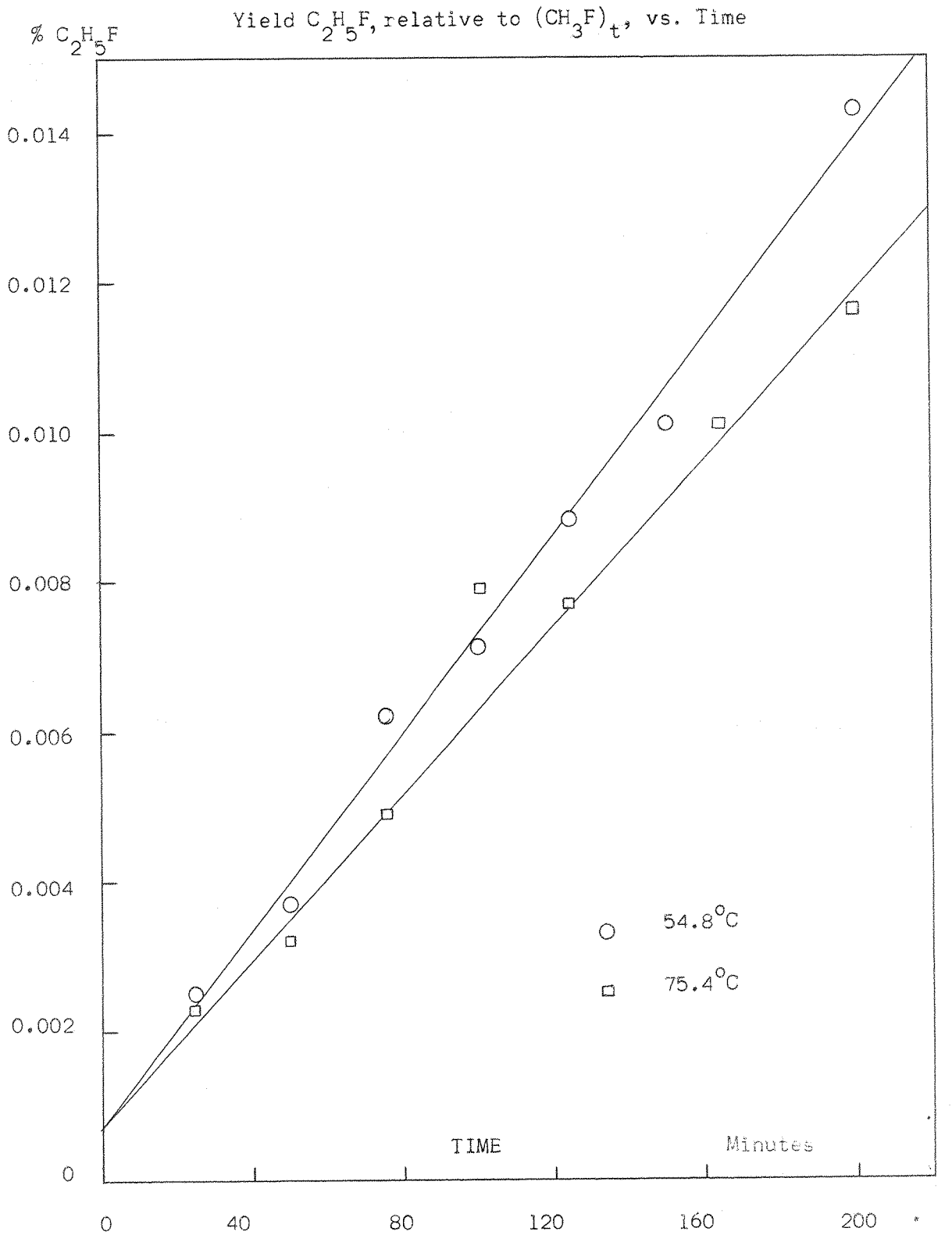
Yield C_2H_5F, relative to $(CH_3F)_t$, vs. Time
% C_2H_5F
0.014
0.012
0.010
0.008
0.006
0.004
0.002
0
TIME
Minutes
0
40
80
120
160
200
54.8°C
75.4°C

FIGURE 16.

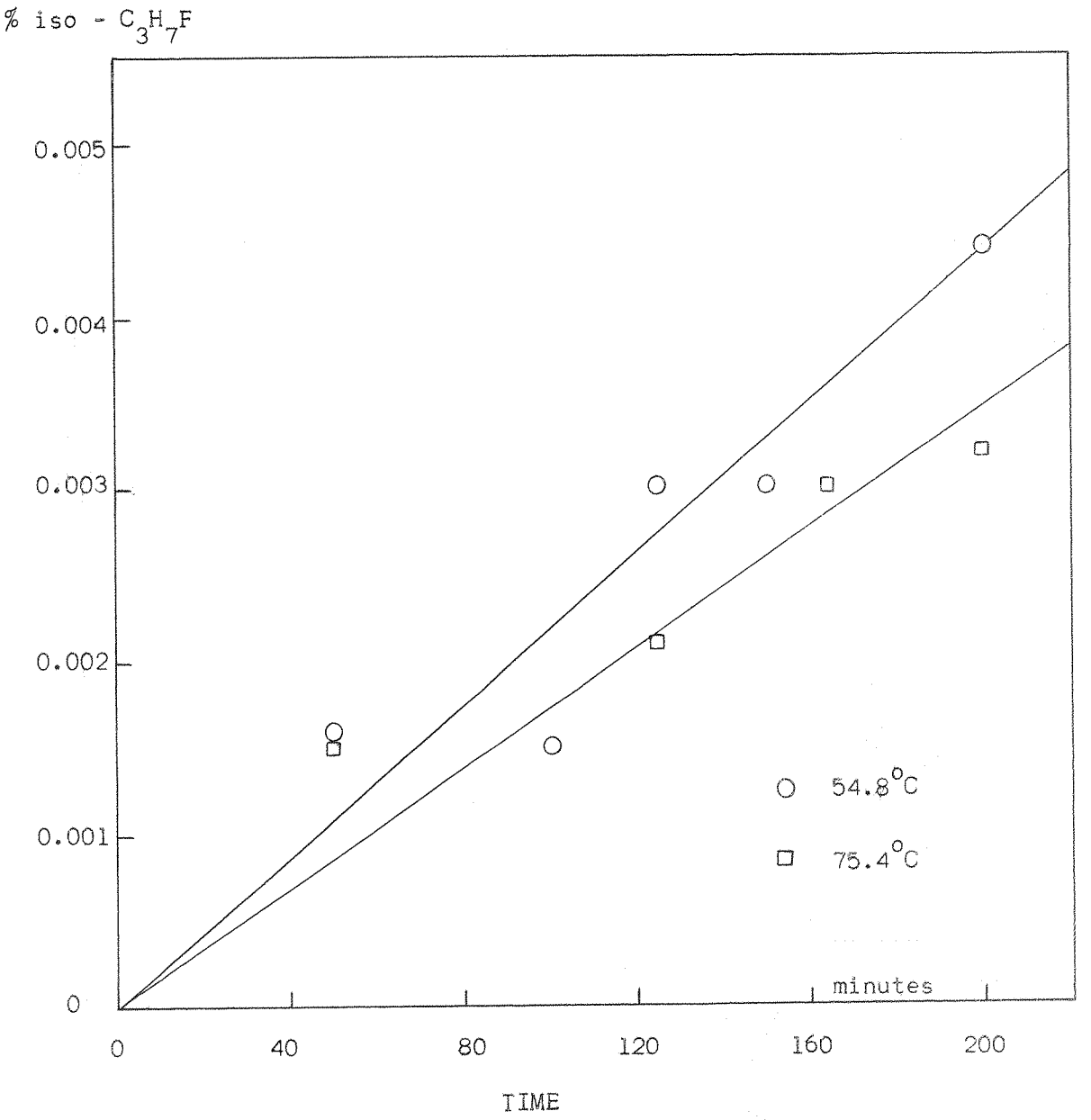

Yield iso - C_3H_7F , relative to $(CH_3F)_t$, vs. Time

FIGURE 17.

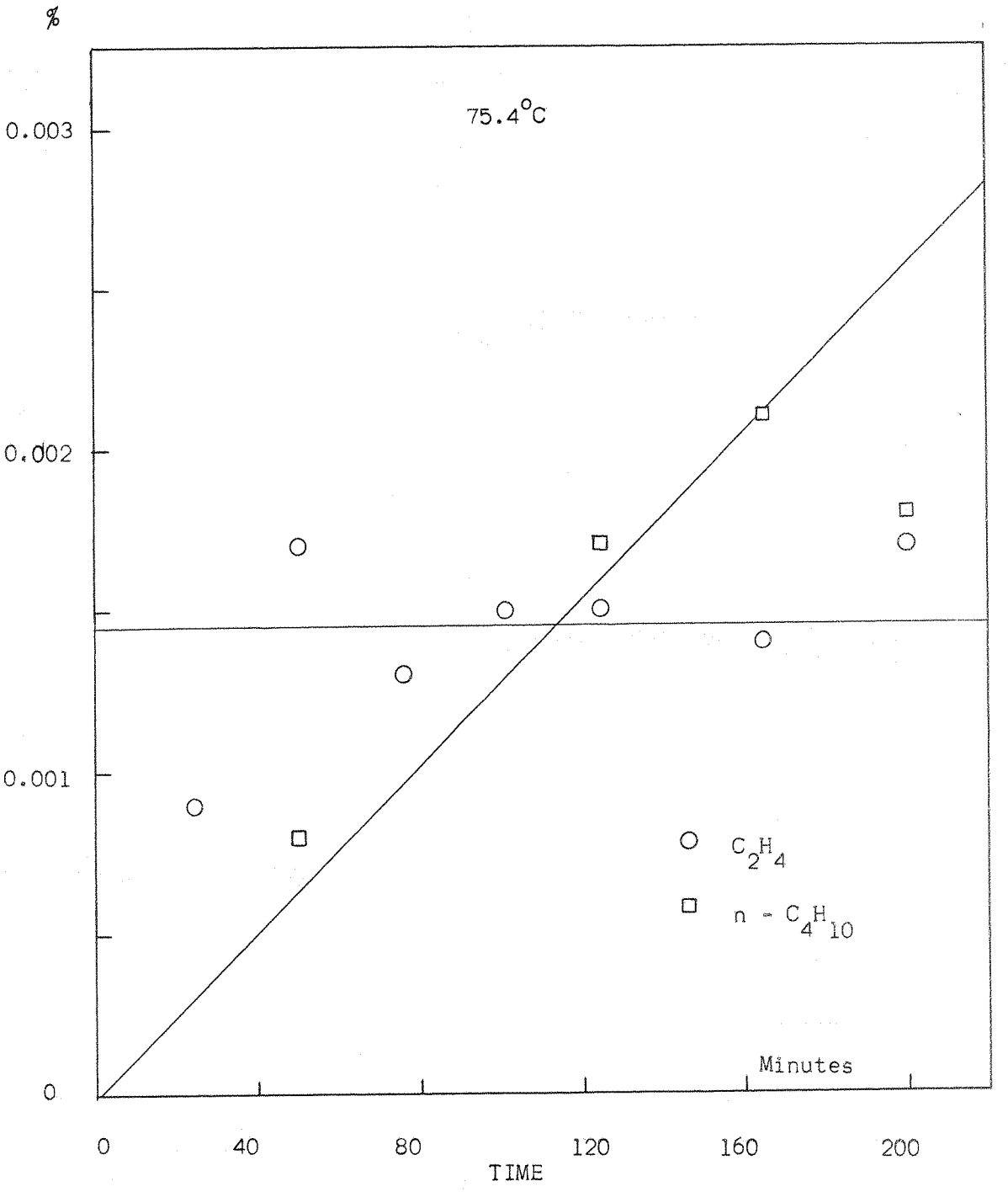

Yield C_2H_4 and n - C_4H_{10} vs. Time.(CH_3F)

FIGURE 18.

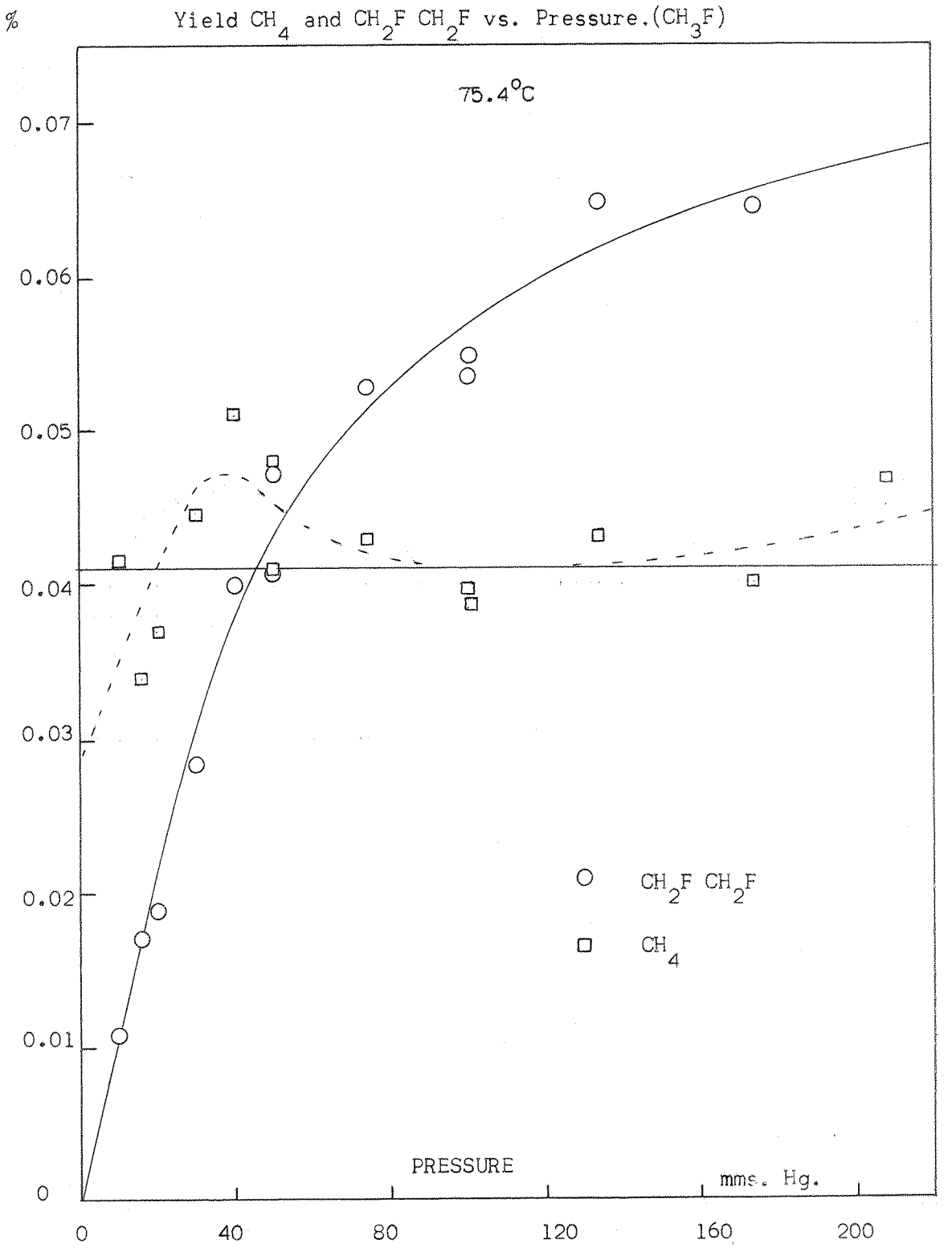
%
Yield CH_4 and CH_2F CH_2F vs. Pressure.(CH_3F)
75.4°C
0.07
0.06
0.05
0.04
0.03
0.02
0.01
0
CH_2F CH_2F
CH_4
PRESSURE
mms. Hg.
0
40
80
120
160
200

FIGURE 19

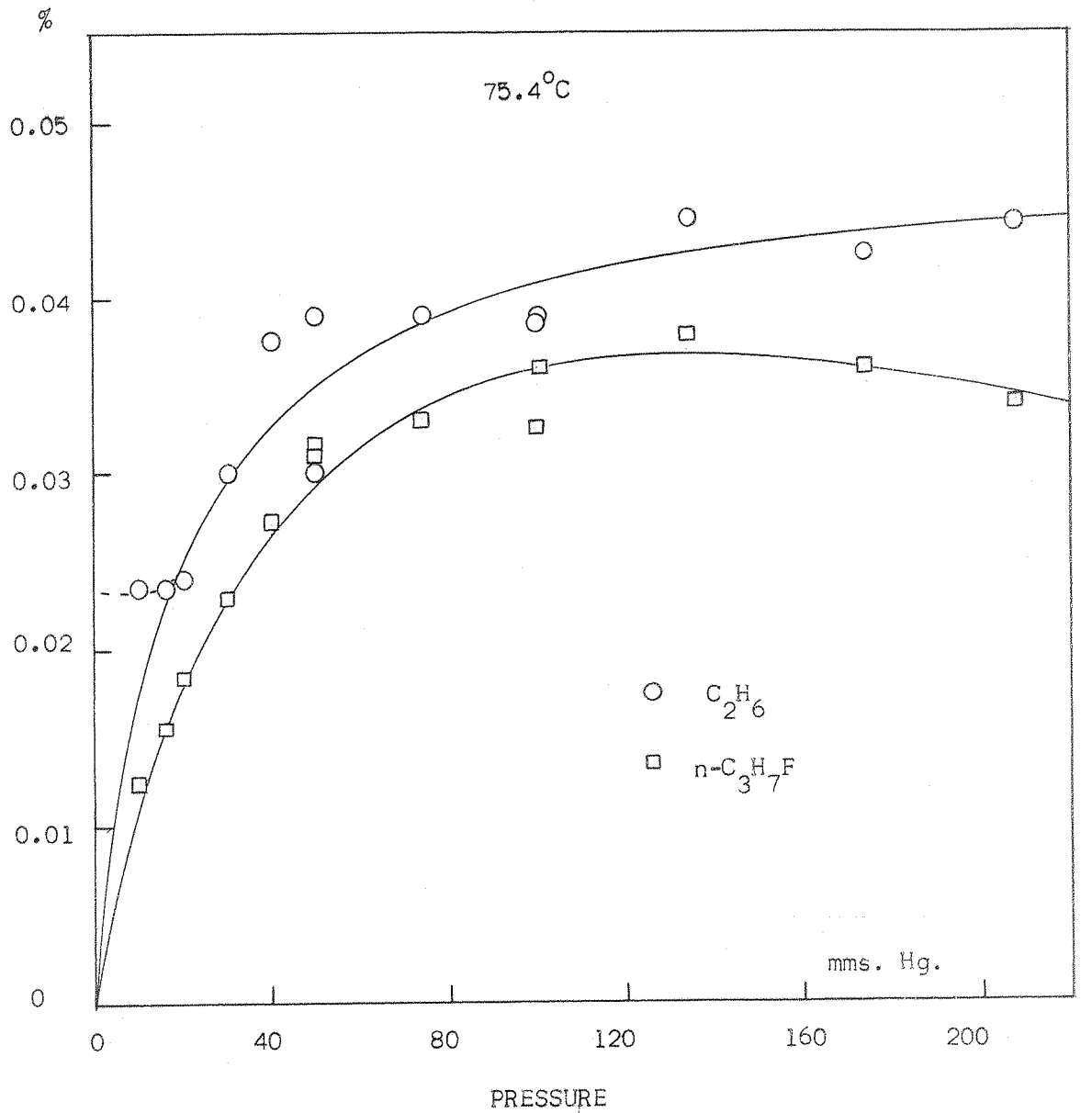

Yield C_2H_6 and n - C_3H_7F vs. Pressure.(CH_3F)

FIGURE 20

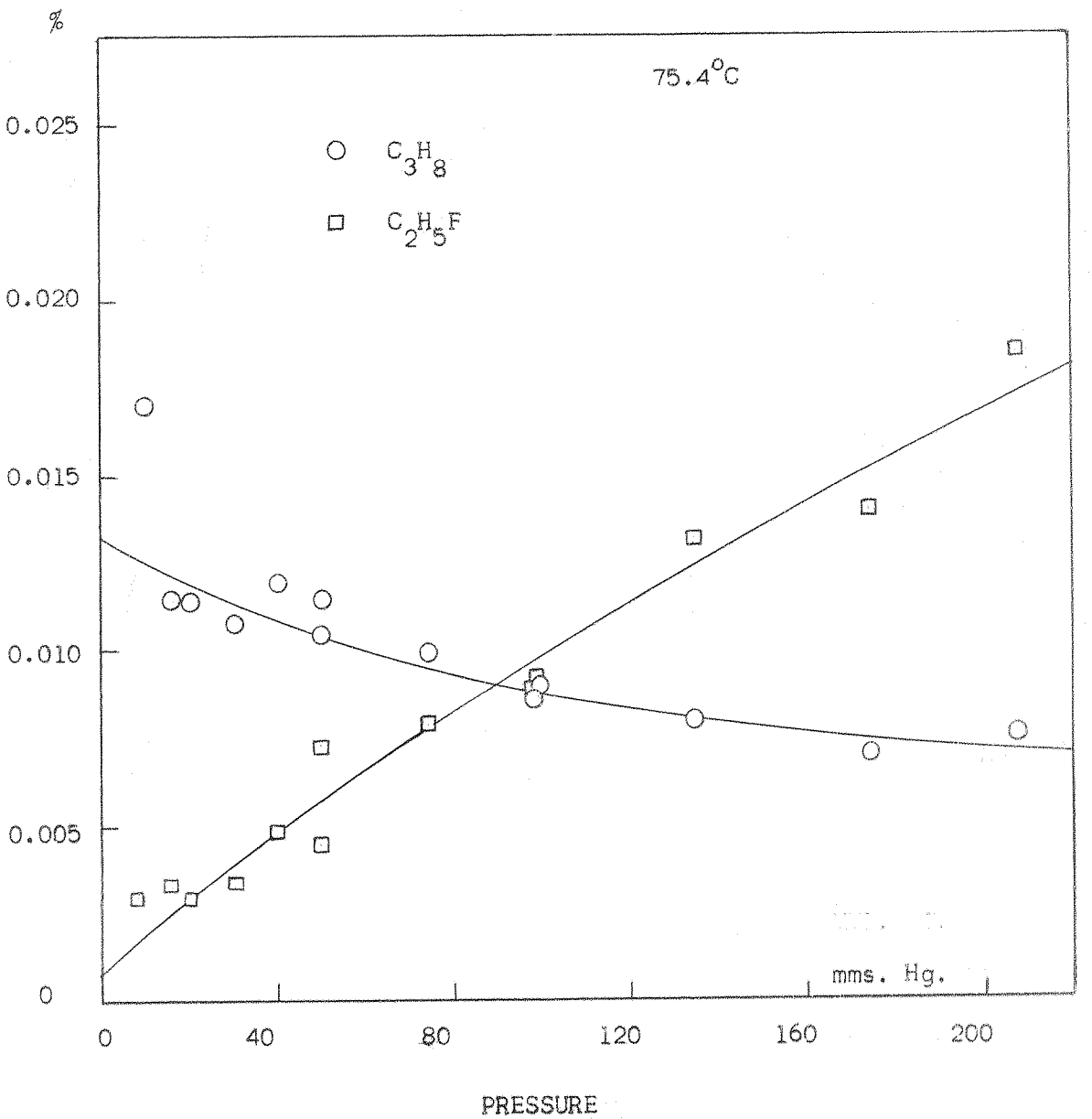

Yield C_3H_8 and C_2H_5F vs. Pressure.(CH_3F)

FIGURE 21

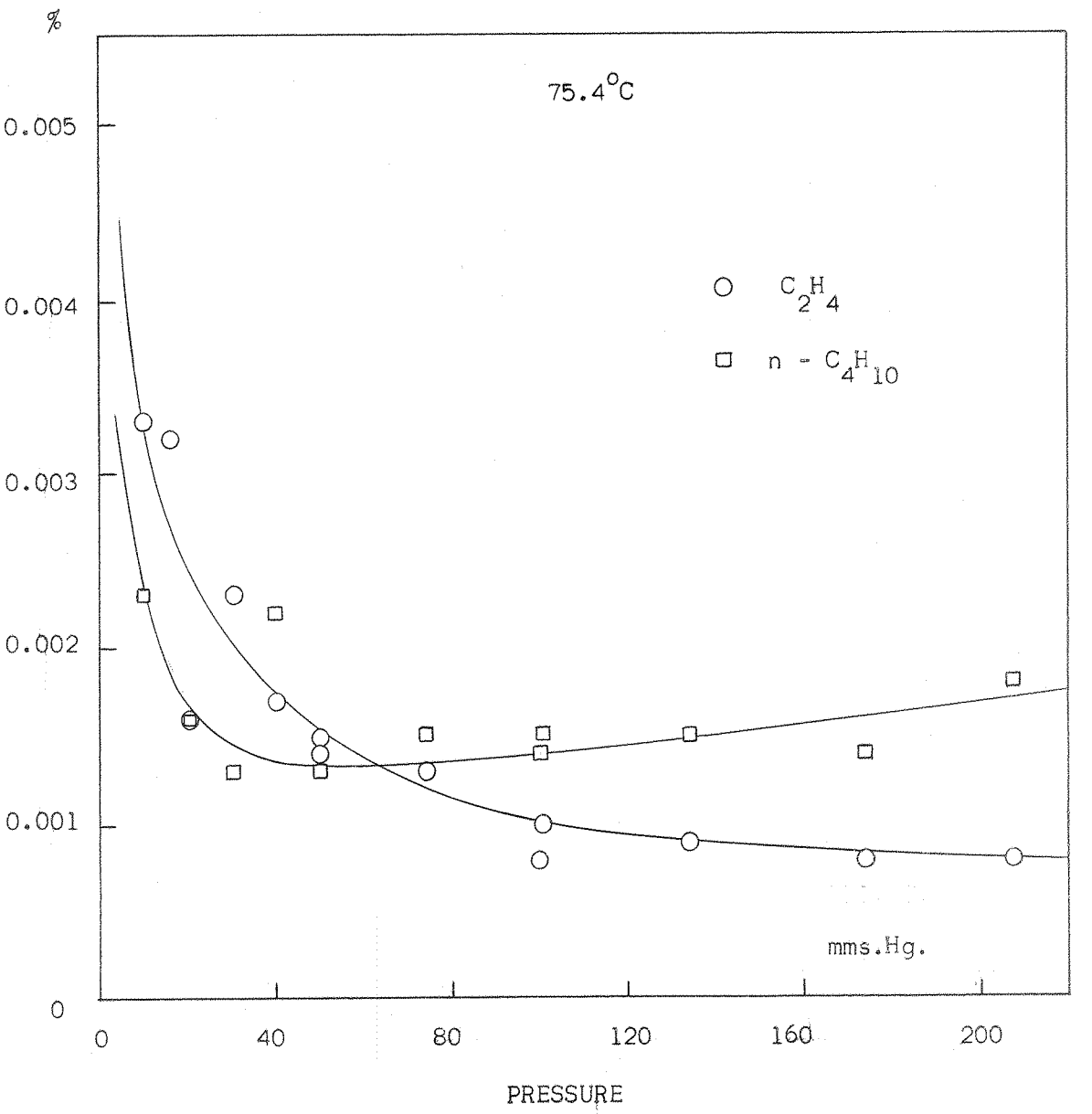

Yield C_2H_4 and n - C_4H_{10} vs. Pressure.(CH_3F)

FIGURE 22

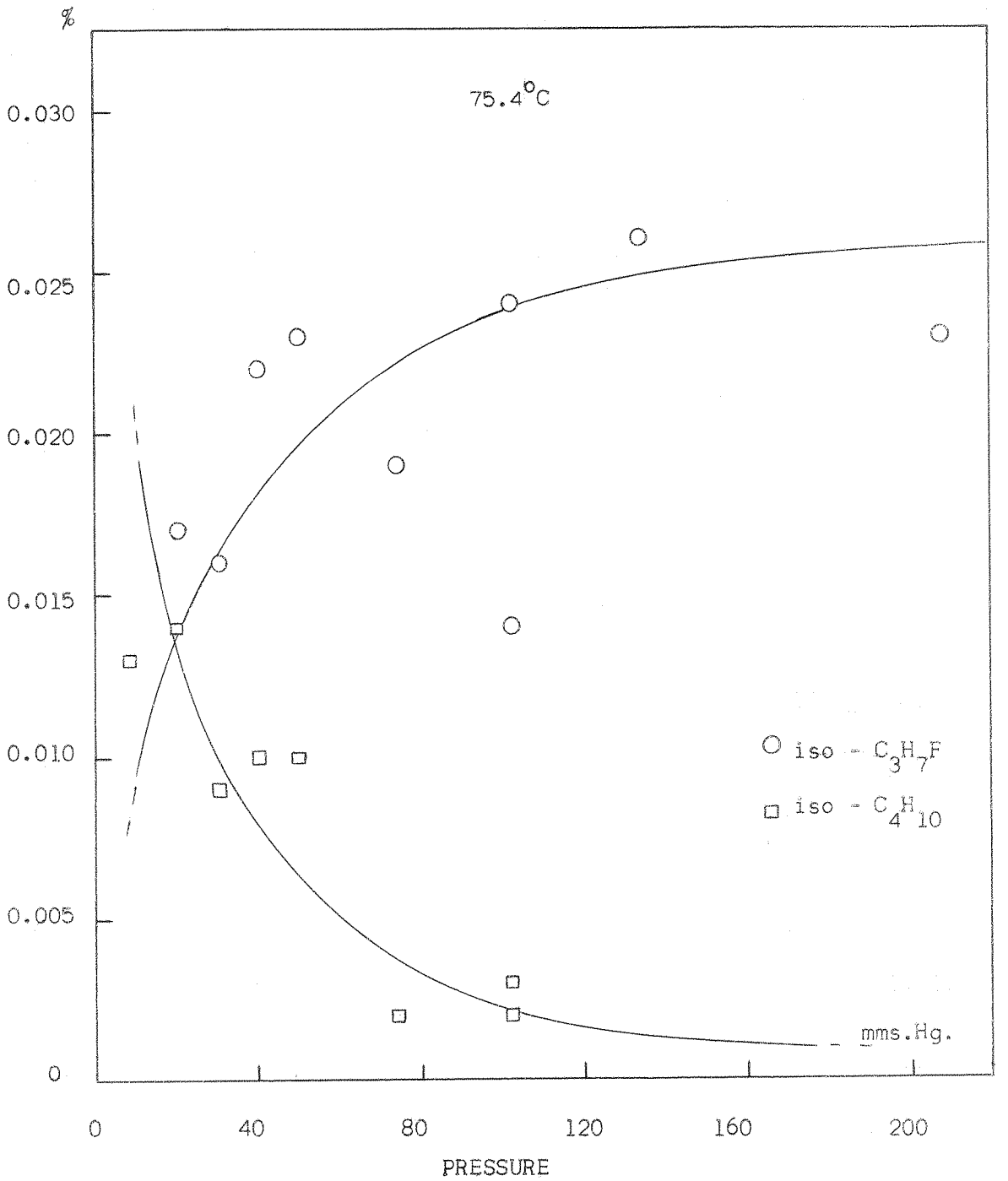

Yield iso - C_3H_7F and iso - C_4H_{10} vs. Pressure

FIGURE 23.

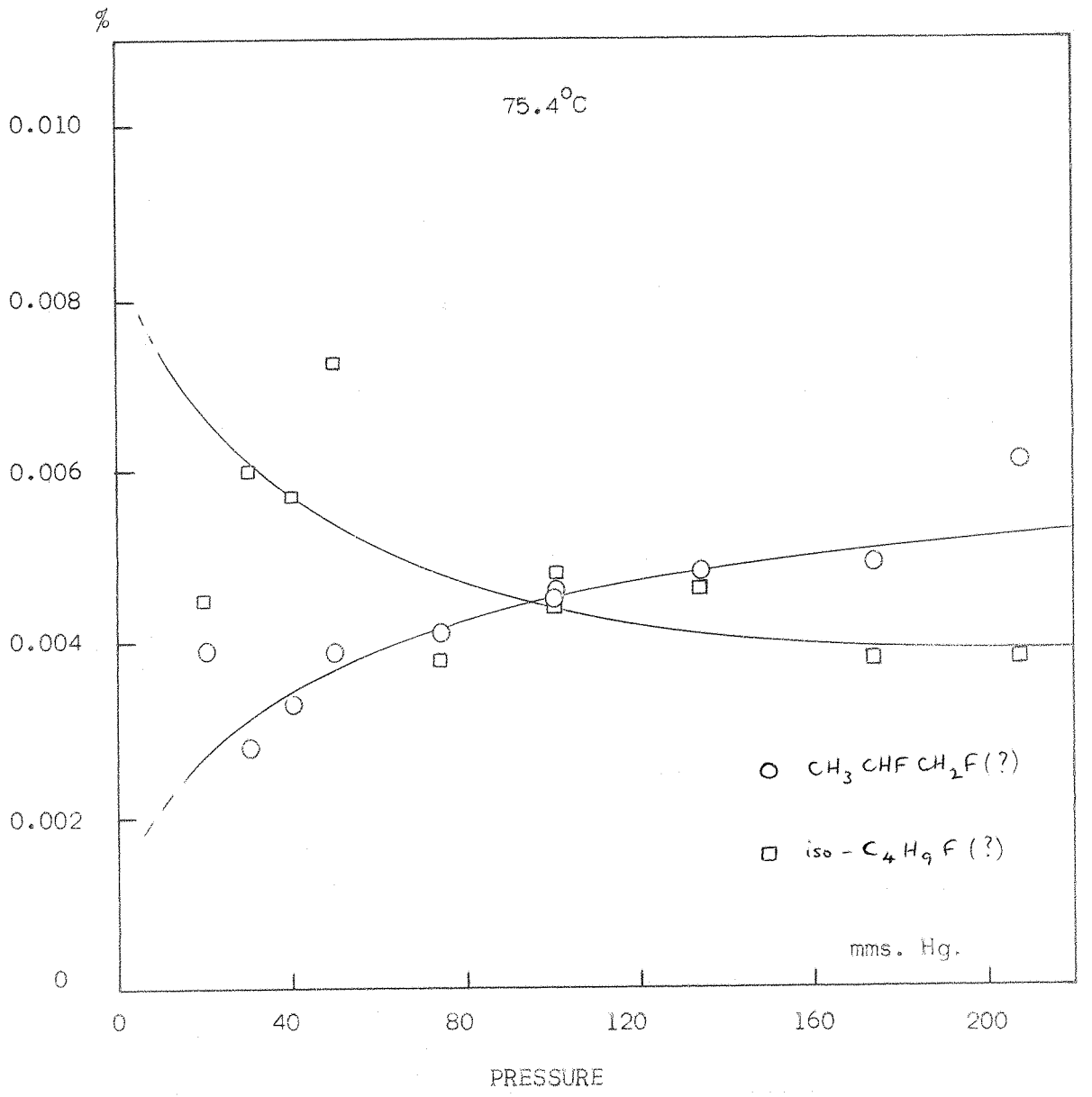

Yield CH_3CHFCH_2F(?) and iso-C_4H_9F(?) vs. Pressure

C H A P T E R IV

DISCUSSION

(a) The Fluoroform/Hydrogen System

Due to the very small quenching cross-section of fluoroform, the only quenching step of importance in this system (and in all other fluoromethane/hydrogen systems) is:

$$Hg^* + H_2 \longrightarrow Hg + H + H \quad . \qquad (1)$$

The quenching efficiency of hydrogen is high and non-dissociative quenching processes may be considered unimportant. The hydrogen atoms can either recombine in a termolecular collision or abstract the hydrogen atom from fluoroform:

$$H + H + M \longrightarrow H_2 + M \quad , \qquad (2)$$

$$H + CHF_3 \longrightarrow H_2 + CF_3 \quad . \qquad (3)$$

The possibility of fluorine abstraction has been discounted on the grounds that the expected activation energy would be much higher than for hydrogen abstraction and very few examples of fluorine abstraction have been reported.[22]

The following recombination reactions are then possible:

$$CF_3 + CF_3 \longrightarrow C_2F_6 \quad , \qquad (4)$$

$$H + CF_3 \longrightarrow CHF_3^* \quad . \qquad (5)$$

(The reversibility of (4) is assumed to be negligible at 50 mms. Hg). Considering the radical and atom concentrations, reaction (5) will be much faster than (4), producing a molecule with at least 106 Kcal.mole^{-1} excitation energy. The activation energy for hydrogen

fluoride elimination from fluoroform has been estimated [23] to be about 76 Kcal.mole^{-1}, from shock tube measurements of its thermal decomposition [18]. Although this value is subject to some uncertainty, the chemically activated molecule formed in (5) must contain 30 Kcal.mole^{-1}, or more, in excess of that required for reaction (6):

$$CHF_3^* \longrightarrow {}^1CF_2 + HF \quad . \qquad (6)$$

The observed absence of CDF_3 in the CHF_3/D_2 runs suggests that collisional deactivation of this excited molecule is very slow compared to the rate of its decomposition under the conditions studied. In view of the large energy contained in these molecules and the few degrees of freedom among which it can be distributed, this high rate of elimination is to be expected.[23]

It has been reported [19a,d] that difluoromethylene does not react with molecular hydrogen in the gas phase (c.f. methylene and molecular hydrogen [24]). Since hydrogen atoms are abundant in this system, it seems reasonable to suppose that addition of two hydrogen atoms could occur:

$$H + {}^1CF_2 \longrightarrow CHF_2 \quad , \qquad (7)$$

$$H + CHF_2 \longrightarrow CH_2F_2^* \quad . \qquad (8)$$

The insertion reaction of difluoromethylene with fluoroform (9), reported in shock tube studies [18], does not appear to be important here:

$$CHF_3 + {}^1CF_2 \longrightarrow CHF_2 \cdot CF_3^* \quad . \qquad (9)$$

The product of reaction (8) is again chemically activated (by about 103 Kcal.mole^{-1}) and will rapidly eliminate hydrogen fluoride as in the activated fluoroform:

$$CH_2F_2^* \longrightarrow :CHF + HF. \quad (10)$$

Assuming that monofluoromethylene reacts in a similar way to difluoromethylene, the following reactions are possible:

$$H + :CHF \longrightarrow CH_2F \quad (11)$$

$$H + CH_2F \longrightarrow CH_3F^* \quad (12)$$

$$CH_3F^* \longrightarrow :CH_2 + HF \quad (13)$$

$$H + :CH_2 \longrightarrow CH_3 \quad (14)$$

$$H + CH_3 \rightleftharpoons CH_4^* \quad (15)$$

$$H_2 + :CH_2 \longrightarrow CH_4^{**} \quad (16)$$

$$CH_4^{**} \longrightarrow CH_3 + H \quad (17)$$

$$M + CH_4^* \text{ (or } CH_4^{**}) \longrightarrow CH_4 + M \quad (18)$$

Since methylene is known to react with hydrogen[24], reactions (16) and (17) may be important. It is assumed that hydrogen fluoride elimination from $CH_2F_2^*$ and CH_3F^* is much faster than collisional deactivation by reactions (19) and (20), confirmed by the low yields of the stabilized molecules:

$$CH_2F_2^* + M \longrightarrow CH_2F_2 + M \quad (19)$$

$$CH_3F^* + M \longrightarrow CH_3F + M \quad (20)$$

From the above scheme it can be seen that CF_3 and CH_3 are the most likely radicals to be involved in recombination reactions, so that in addition to (4), the following reactions will be important:

$$CH_3 + CH_3 \longrightarrow C_2H_6 \qquad (21)$$

$$CH_3 + CF_3 \longrightarrow CH_3.CF_3^* \qquad (22)$$

$$CH_3.CF_3^* \longrightarrow CH_2 = CF_2 + HF \qquad (23)$$

$$CH_3.CF_3^* + M \longrightarrow CH_3.CF_3 + M \ . \qquad (24)$$

The reverse of (21) is again unimportant at the pressure studied. Reactions (22) — (24) were first studied in the co-photolysis of acetone and hexafluoroacetone.[11] No 1,1- difluoroethylene would be expected in the products since hydrogen addition to olefins will be rapid.

The presence of all the identified products is therefore explained by the above mechanism. Reaction (15) is the only case considered where an activated molecule can decompose by a process which is the reverse of its formation, since activated molecules containing fluorine have been assumed to decompose only by elimination of hydrogen fluoride. However, the redissociation of CHF_2, CH_2F and CH_3 radicals, by the reverse of reactions (7), (11) and (14) respectively, may be important, since these radicals will be vibrationally "hot". Although this will only have the effect of reducing the rate the relevant forward reactions, as far as the above mechanism is concerned, it increases the probability of

dimerization of methylenes, e.g.

$$:CF_2 + :CF_2 \longrightarrow C_2F_4 \quad .$$

Sequential addition of hydrogen and elimination of hydrogen fluoride may then follow (see below), finally yielding ethane and methane. This will similarly apply to the mechanisms proposed for the following systems. However, owing to the high concentration of hydrogen atoms, dimerization of methylenes is considered to be insignificant compared to hydrogen atom addition.

It has been assumed throughout that all hydrogen fluoride, produced in the elimination steps of this and the following mechanisms, reacts rapidly with the quartz walls of the reaction vessel and hence plays no major role in reactions other than:

$$SiO_2 + 4HF \longrightarrow SiF_4 + 2H_2O \quad .$$

The presence of silicon tetrafluoride in the reaction products of this system was confirmed by infra-red and mass spectrometry.

As already mentioned, the retention times of ethane and hexafluoroethane were very similar, under the conditions used, for both the alumina and silica gel columns (see also Appendix 1). Although the peak ascribed to ethane was never observed to possess a shoulder, it is probable that this peak, obtained with the flame ionization detector, contained a significant contribution from C_2F_6. The detector sensitivity for C_2F_6 is about 150 times less than that for ethane.

The fact that no methane was observed in the C_2F_4/H_2 runs

where a small proportion of hydrogen was used does suggest that direct addition of molecular hydrogen to difluoromethylene is slow, if it occurs at all. However, the appearance of methane and ethane when a large excess of hydrogen was present can be explained by the following mechanism, which does not include reactions (7) and (8) above:

$$C_2F_4 + H \longrightarrow CHF_2.CF_2$$

$$CHF_2.CF_2 + H \longrightarrow CHF_2.CHF_2^* \quad (i)$$

$$CHF_2.CHF_2^* \longrightarrow C_2F_3H + HF \quad (ii)$$

$$CHF_2.CHF_2^* + M \longrightarrow C_2H_2F_4 + M$$

$$C_2F_3H + 2H \longrightarrow CH_2F.CHF^*$$

$$CH_2F.CHF^* \longrightarrow C_2H_2F_2 + HF$$

This process continues until:

$$C_2H_4 + 2H \longrightarrow C_2H_6^*$$

$$C_2H_6^* \longrightarrow CH_3 + CH_3$$

$$C_2H_6^* + M \longrightarrow C_2H_6 + M$$

$$CH_3 + H + M \longrightarrow CH_4 + M.$$

The rate of elimination of hydrogen fluoride from excited $CHF_2.CHF_2$ formed by the recombination of CHF_2 radicals has been shown [25] to be very slow under the present conditions. However, since $CHF_2.CHF_2^*$ is vibrationally excited by the formation of the stronger C - H bond in reaction (i), elimination by (ii) may be

significant. Subsequent hydrogen addition and hydrogen fluoride eliminations will then lead to ethane and methane.

Due to incomplete analysis and uncertainties in the proposed mechanism, too much significance could not be placed on kinetic data determined from CHF_3/H_2 results. However, it seems reasonable to suppose that reaction (3) involves the largest activation energy and is the rate determining step in the formation of methane, at least at the lower temperatures; i.e.:

$$d[CH_4]/dt = k_3[CHF_3][H].$$

From figure (3) it can be seen that the rate of methane formation is approximately linear at temperatures less than 150°C and for irradiation times less than 120 minutes. Therefore:

$$[CH_4]/[CHF_3]_t = k_3[H] \times t \text{ , at time } t.$$

Assuming the hydrogen atom concentration to remain unchanged, the percentage yield of methane at constant time is, then, a measure of k_3. Plotting the points from figure (8) in the form $\log_{10} [CH_4]/[CHF_3]_t$ against the reciprocal of the temperature (°K), as in figure 24, should therefore give a straight line corresponding to the Arrhenius activation energy of reaction (3). The line in fact shows considerable curvature towards higher temperatures, probably for the following reasons:

(a) as the temperature increases, the rate of abstraction of hydrogen by reaction (3) may become comparable with the rate of quenching of Hg ($^3P_1$) by hydrogen, at which point

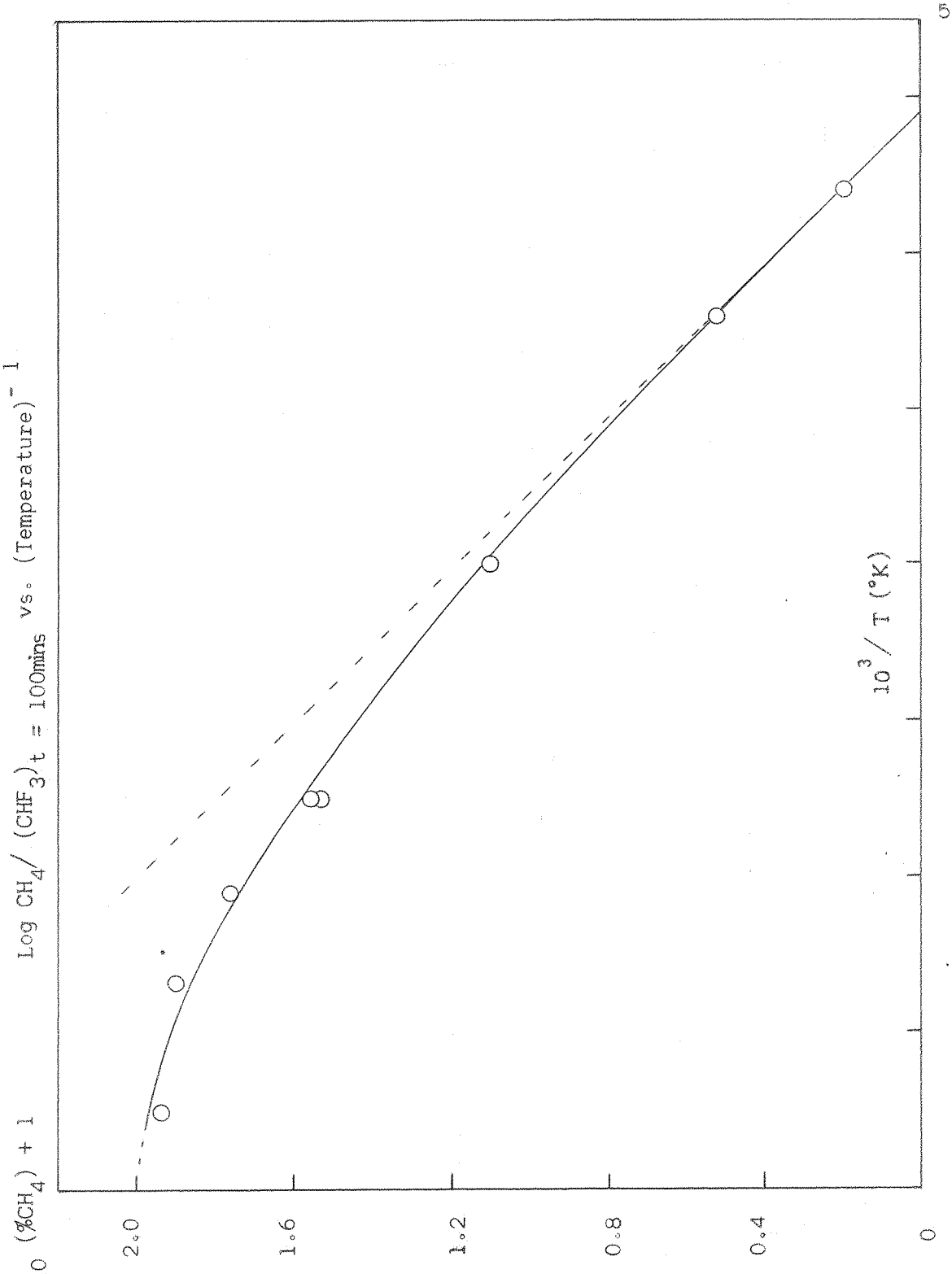
Log10 (%CH4) + 1
Log CH4/ (CHF3)t = 100mins vs. (Temperature)-1
2.0
1.6
1.2
0.8
0.4
0
2.0
2.2
2.4
2.6
2.8
3.0
3.2
3.4
10^3 / T (°K)

FIGURE 24.

(3) is no longer rate determining;

(b) as the methane yield increases with temperature so the competing reaction,

$$CH_4 + H \longrightarrow CH_3 + H_2 \quad , \qquad (25)$$

will become significant; and

(c) as the rate of reaction (3) increases with temperature, so $[H]$ will decrease, since (1) and (2) can be assumed to be temperature independent, and the assumption that $[H]$ is constant is no longer valid.

Nevertheless, the curve appears to approach linearity at the lowest temperatures and the gradient of the tangent to the curve at this point gives a value of 9.4 Kcal.mole^{-1} for the activation energy. A recent estimation[26] of the activation energy of reaction (3) was given as 11.2 $\pm$ 2 Kcal.mole^{-1}. Since the value obtained here will be a minimum, the agreement is good.

(b) The Difluoromethane/Hydrogen System

By analogy with CHF_3/H_2 system, the following mechanism can be written for the reaction of difluoromethane and hydrogen:

$$CH_2F_2 + H \longrightarrow CHF_2 + H_2 \qquad (26)$$

$$CHF_2 + H \longrightarrow CH_2F_2^* \quad . \qquad (8)$$

Reactions (10) - (18), yielding methyl radicals and methane, will occur here, as in the fluoroform system above. The following radical recombination reactions are then possible:

$$CH_3 + CH_3 \longrightarrow C_2H_6 \quad (21)$$

$$CHF_2 + CHF_2 \longrightarrow CHF_2.CHF_2 \quad (27)$$

$$CHF_2 + CHF_2 \longrightarrow CH_2F_2 + :CF_2 \quad (28)$$

$$CH_3 + CHF_2 \longrightarrow CH_3.CHF_2^* \quad (29)$$

$$CH_3.CHF_2^* \longrightarrow CH_2 = CHF + HF \quad (30)$$

$$CH_3.CHF_2^* + M \longrightarrow CH_3.CHF_2 + M \ . \quad (31)$$

The elimination of hydrogen fluoride from $CH_3.CHF_2^*$, formed by reaction (29), has been observed [27] to be rapid. Elimination from $CHF_2.CHF_2$, formed by CHF_2 radical recombination, is very slow under the present conditions [25, 27], and the disproportionation reaction (28) is more important [14, 28].

The appearance of propane and n-butane in the products, indicating a high concentration of ethyl radicals, can be explained by the further reaction of vinyl fluoride produced in reaction (30):

$$CH_2 = CHF + 2H \longrightarrow CH_3.CH_2F^* \quad (32)$$

$$CH_3.CH_2F^* \longrightarrow CH_2 = CH_2 + HF \quad (33)$$

$$CH_2 = CH_2 + H \longrightarrow C_2H_5 \quad (34)$$

$$CH_3 + C_2H_5 \longrightarrow C_3H_8 \quad (35)$$

$$C_2H_5 + C_2H_5 \longrightarrow n\text{-}C_4H_{10} \ . \quad (36).$$

Although an increase in reaction rate with temperature was observed (Fig.(9), insufficient data was obtained to enable an estimate of the activation energy for reaction (26) to be determined.

A fall-off in the rate of methane formation was also observed at higher temperatures, suggesting that the competing hydrogen abstraction from methane is also important here,

$$H + CH_4 \longrightarrow CH_3 + H_2 , \qquad (25)$$

or that the rate of quenching by hydrogen is becoming the rate determining step.

(c) The Methyl Fluoride/Hydrogen System

The preliminary investigations carried out on this system were complicated by the presence of an impurity in the methyl fluoride that was not separated by the silica gel or alumina columns used in the analysis. However, the later run with purified reactant showed a qualitative agreement. The apparent drop in methane yield with an increase in temperature, and an accompanying increase in ethane yield, are again probably due to the competing secondary reaction (25);

$$H + CH_4 \longrightarrow CH_3 + H_2 . \qquad (25)$$

The mechanism for the formation of methane will be analogous to that proposed for the previous systems, i.e.,

$$H + CH_3F \longrightarrow CH_2F + H_2 , \qquad (37)$$

followed by reactions (12) to (18) above.

The detection of propane, n-butane, and n-propyl fluoride again indicates a significant concentration of ethyl radicals, formed by the following steps:

$$CH_2F + CH_2F \longrightarrow CH_2F.CH_2F^* \quad (38)$$

$$CH_2F.CH_2F^* \longrightarrow CH_2 = CHF + HF \quad (39)$$

$$CH_2 = CHF + H \longrightarrow CH_3.CHF \quad (40)$$

$$CH_3.CHF + H \longrightarrow CH_3CH_2F^* \quad (41)$$

$$CH_3 + CH_2F \longrightarrow CH_3CH_2F^{**} \quad (42)$$

$$CH_3CH_2F^*(\text{or } CH_3CH_2F^{**}) \longrightarrow CH_2 = CH_2 + HF \quad (33)$$

$$CH_2 = CH_2 + H \longrightarrow C_2H_5 \cdot \quad (34)$$

The chemically activated fluoroethanes produced in reactions (38), (41) and (42) are also capable of undergoing collisional deactivation. ($CH_3.CH_2F^*$ is a "hotter" molecule than $CH_3.CH_2F^{**}$ and hence eliminates hydrogen fluoride at a faster rate).

Radical recombination steps can then lead to the observed products:

$$CH_3 + CH_3 \longrightarrow C_2H_6 \quad (21)$$

$$CH_3 + C_2H_5 \longrightarrow C_3H_8 \quad (35)$$

$$C_2H_5 + C_2H_5 \longrightarrow n\text{-}C_4H_{10} \cdot \quad (36)$$

Disproportionation reactions for methyl+ethyl and ethyl+ethyl radicals[29] will also occur, but to a lesser extent, along-side reactions (35) and (36):

$$C_2H_5 + CH_2F \longrightarrow n\text{-}C_3H_7F^* \quad (43)$$

$$CH_3CHF + CH_3 \longrightarrow \text{iso - } C_3H_7F^* \cdot \quad (44)$$

The products of reactions (43) and (44) are both chemically

activated and will eliminate hydrogen fluoride (45) (at different rates) unless stabilized by collision:

$$n\text{-}C_3H_7F^* \text{ (or iso-}C_3H_7F^*) \longrightarrow CH_3CH{=}CH_2 + HF \quad (45)$$

$$CH_3.CH{=}CH_2 + H \longrightarrow CH_3.CH.CH_3 \quad (46)$$

$$CH_3.CH.CH_3 + CH_3 \longrightarrow \text{iso-}C_4H_{10} . \quad (47)$$

The formation of iso-butane is thus explained by (45) - (47).

The possibility of insertion by methylene into the C-H bond of methyl fluoride [27] was not considered important here since high concentrations of hydrogen and hydrogen atoms are present:

$$:CH_2 + CH_3F \longrightarrow CH_3CH_2F^{***}. \quad (48)$$

(d) Quenching by Methyl Fluoride

Although the mercury photosensitized decomposition of paraffins has been extensively studied for several decades, the precise quenching mechanisms involved are still not fully understood. The existence of a collision complex, (HgM)*, has been postulated by some investigators and evidence for its existence in several systems has been found [30]. The following mechanism includes all processes that have been proposed to occur in quenching by a typical paraffin, M; [31]

$$Hg + h\nu\ (2537\text{Å}) \longrightarrow Hg^*$$

$$Hg^* \longrightarrow Hg + h\nu \quad (a)$$

$$Hg^* + M \longrightarrow (HgM)^* \quad (b)$$

$$(HgM)^* \longrightarrow Hg^* + M \quad (-b)$$

$$(HgM)^* \begin{cases} \longrightarrow Hg + M + h\nu' & (c) \\ \longrightarrow Hg' + M' & (d) \\ \longrightarrow Hg + R + H & (e) \end{cases}$$

where $h\nu'$ denotes a quantum of light of wavelength other than 2537Å;

Hg, Hg' and Hg* denote ground state (^1S_o), metastable (^3P_o), and excited ($^3P_1$) mercury atoms respectively; and M' denotes a rotationally or vibrationally excited species.

A plot of the percentage decomposition of methyl fluoride against time is shown in Figure 25. These straight line plots correspond to quantum yields for decomposition of 1.59×10^{-2} and 1.44×10^{-2} at 55°C and 75°C respectively. The variation of percentage decompositon with pressure of reactant is shown in Figure 26.

In terms of the above quenching mechanism, the rate of chemical quenching by methyl fluoride is, $\frac{k_b k_e [CH_3F][Hg^*]}{k_{-b} + k_c + k_d + k_e}$.

The light input to the reaction vessel, in (gm. - atoms Hg*). litre^{-1}, is given by the equation:

$$I_{abs} = \left(k_a + k_b [CH_3F] \cdot \frac{k_c + k_d + k_e}{k_{-b} + k_c + k_d + k_e} \right) \cdot [Hg^*] \qquad (1)$$

Since the quantum yield is small, i.e. $k_a \gg k_b [CH_3F]$, equation (1) reduces to: $I_{abs} \simeq k_a [Hg^*]$.

FIGURE 25

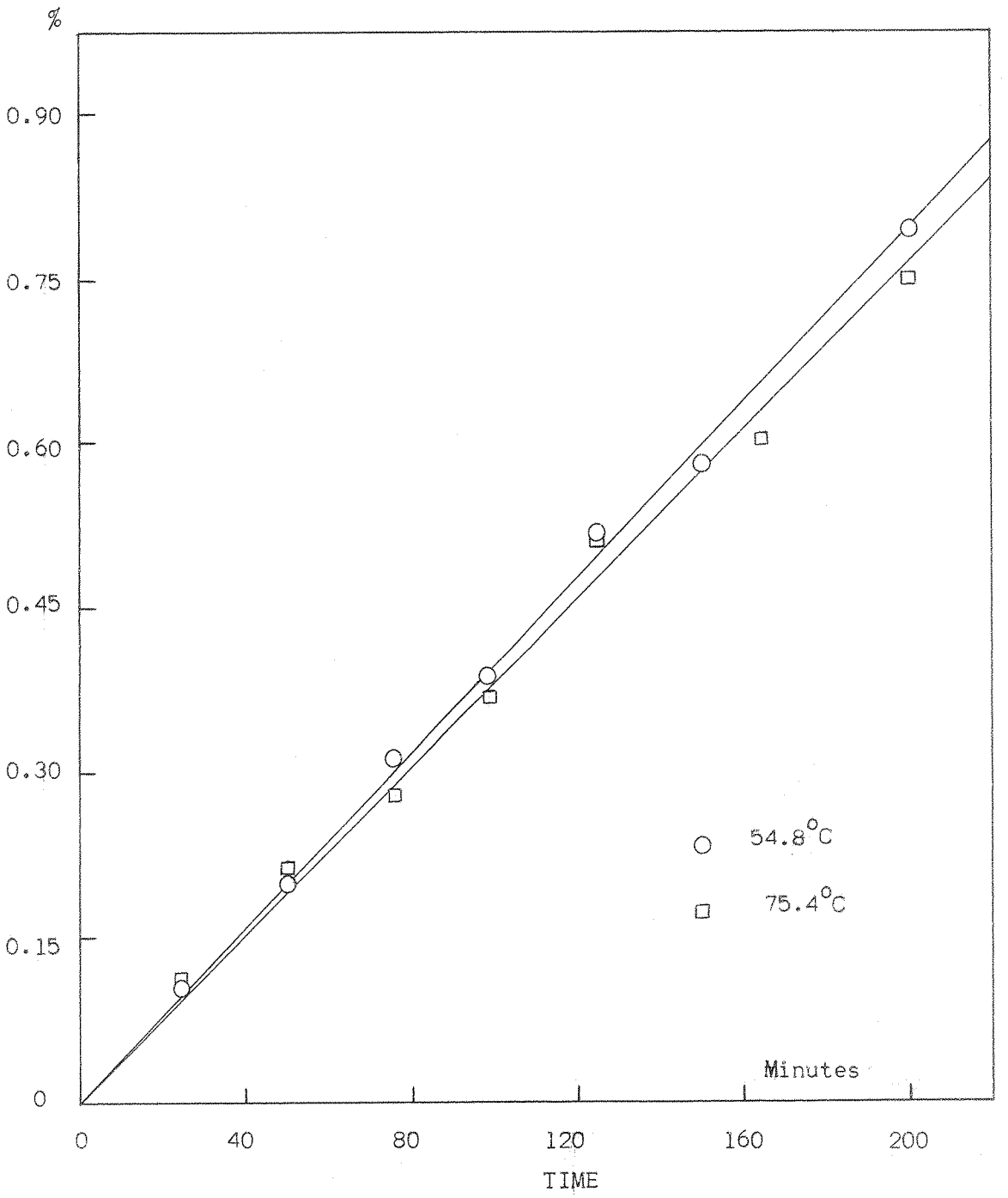

% Decomposition vs. Time.(CH_3F)

FIGURE 26

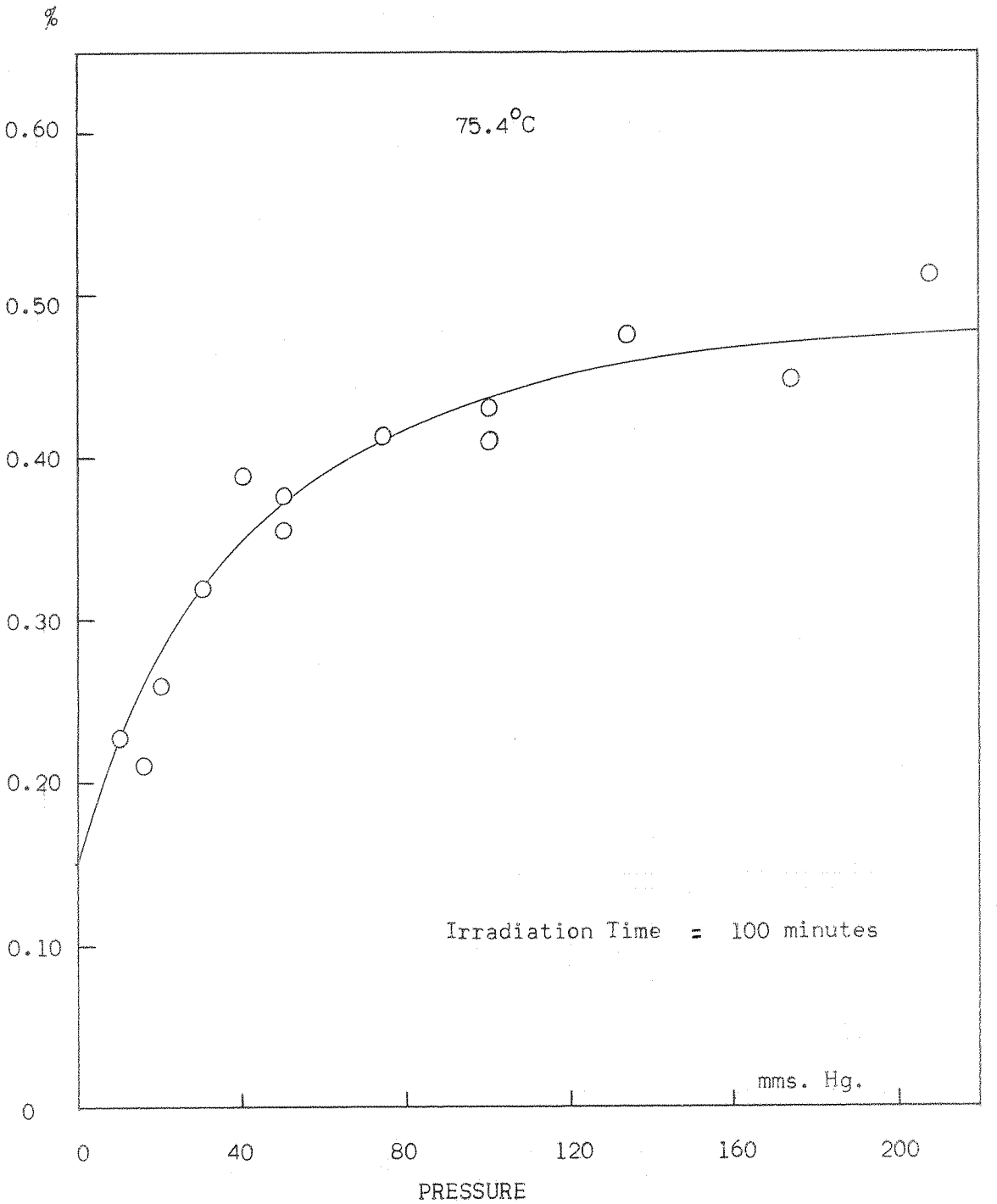

% Decompositon vs. Pressure. (CH_3F)

This predicts that the percentage decomposition, at a given time, will be independent of pressure of reactant. The observed fall-off in percentage decomposition at low pressures (Figure 26) was originally thought to be due to an alternative mode of quenching of Hg*, i.e. by olefins.

Since the rate of collisional stabilization of chemically activated molecules containing fluorine decreases as the pressure decreases, the concentration of olefins, formed by hydrogen fluoride elimination from these molecules, is expected to increase correspondingly (see Figure 21). The chemical quenching efficiencies of olefins are high (k_Q for ethylene is 30×10^{10} l.mole.$^{-1}$ sec.$^{-1}$) [32], and it was thought that a possible reason for the fall-off with pressure was due to quenching by olefins (C_2H_4, $CH_2 = CHF$ and C_3H_6) competing with the resonance phosphorescence reaction (a). However, the rate of quenching by the observed concentration of ethylene at 100 mms.Hg. can be shown to be at least 100 times less than the rate of resonance phosphorescence, and hence is insignificant.

An alternative explanation for the drop in decomposition rate at low pressure would be the occurrence of Lorentz collision broadening of the absorption line [33]. The Doppler half-width of the resonance radiation of a low-pressure mercury lamp is several times that of the absorption line. The addition of a foreign gas to the absorbing medium sharply increases the light absorption due to collision broadening of the absorption line.

Although this Lorentz collision broadening is probably present in this system, it will be shown below that the shape of the pressure dependence can be adequately explained in terms of alternative decomposition path, not directly involving quenching of Hg* ($^3P_1$), which increases with increasing pressure of methyl fluoride.

When CH_2F radicals (formed in the direct quenching reaction (49)) recombine, they produce an activated 1, 2 - difluoroethane molecule which will eliminate hydrogen fluoride unless collisionally stabilized:

$$CH_3F + Hg^* \longrightarrow CH_2F + H + Hg \qquad (49)$$

$$CH_2F + CH_2F \longrightarrow CH_2F.CH_2F^* \qquad (38)$$

$$CH_2F.CH_2F^* \longrightarrow CH_2 = CHF + HF \qquad (39)$$

$$CH_2F.CH_2F^* + M \longrightarrow CH_2F.CH_2F + M. \qquad (50)$$

The rate of formation of stabilized molecules is given by the equation:

$$R_{50} = k_{50}[M] \cdot k_{38}[CH_2F]^2 / (k_{39} + k_{50}[M]).$$

$$\therefore \quad [CH_2F]^2 / R_{50} = 1/k_{38} + \left(k_{39}/k_{38}\, k_{50}\right).[M]^{-1} \quad . \qquad (2)$$

Therefore, a plot of the left-hand side of equation (2) against the reciprocal of the pressure will give a straight line, for which the ratio of slope-to-intercept equals k_{39}/k_{50}, the elimination-to-stabilization rate constant ratio for $CH_2F.CH_2F^*$. In fact, a reliable measure of the variation $[CH_2F]$ with pressure cannot be obtained, but a plot of $(\%\ CH_2F.CH_2F)^{-1}$ against $[M]^{-1}$, Figure 27,

FIGURE 27

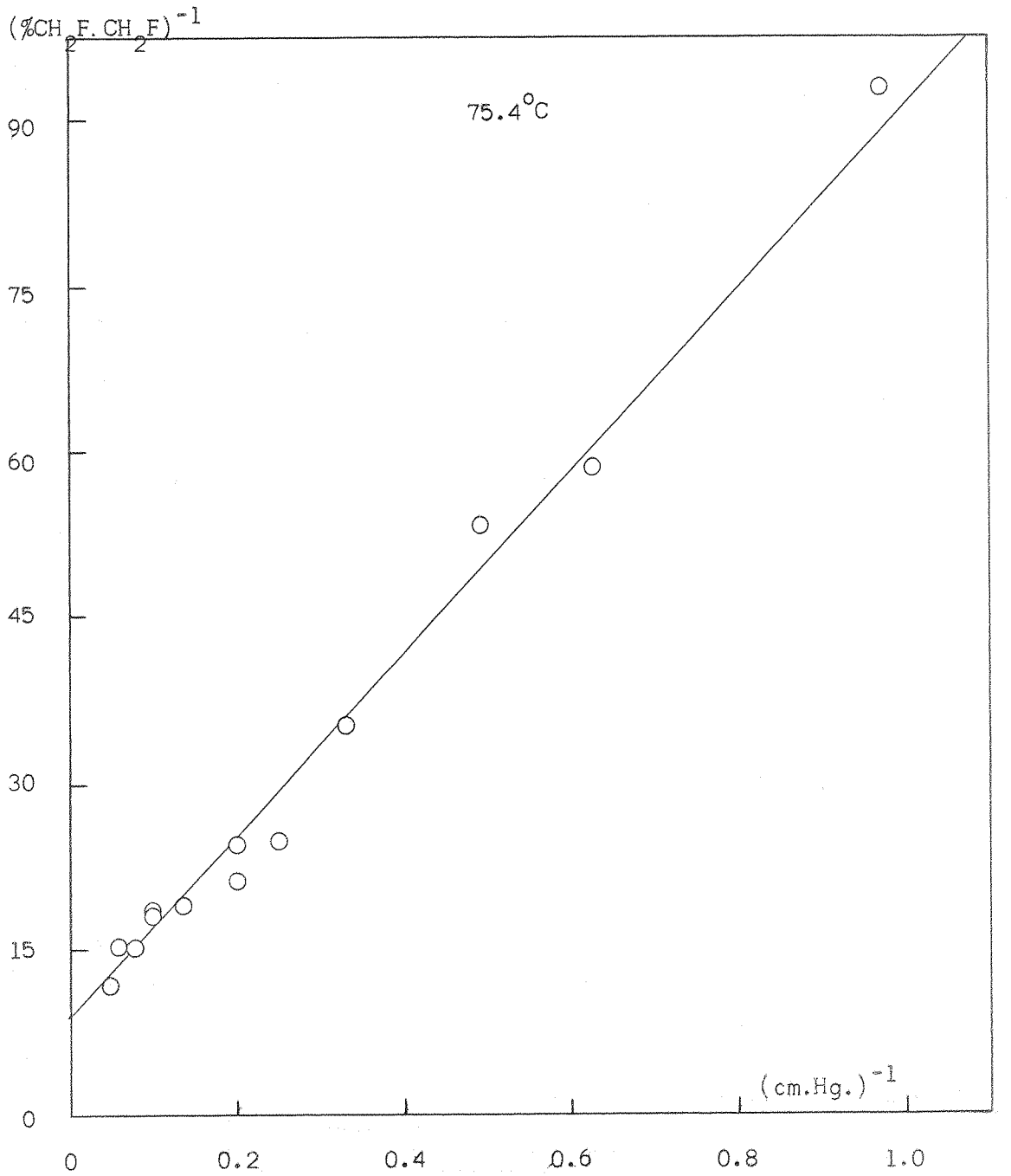

(% CH_2 F CH_2F)$^{-1}$ vs (Pressure)$^{-1}$. (CH_3F)

shows a linear relationship, indicating that $[CH_2F]^2/[M]$ is approximately constant over the pressure range studied. Assuming the constancy of $[CH_2F]^2/[M]$, the straight line of Figure 27 yields a value of about 9.1 cm. for k_{39}/k_{50} at 75°C. Values found for this ratio in the photolysis of fluoroacetones at this temperature are 6.0cm., where $CH_3.CO.CH_2F$ was the deactivating molecule [12], and 2.6 cm., where $CH_2F.CO.CH_2F$ was the deactivating molecule [10,13]. Hence the nature of the deactivating species can be seen to be very important in determining the efficiency with which the "hot" molecule is stabilized by collision.

Using the value of 9.1 cm. for k_{39}/k_{50}, the proportion of $CH_2F.CH_2F^*$ molecules decomposing was found at each pressure studied and hence the percentage decompositon of methyl fluoride occuring via reaction (38). This is shown in Figure 28 (curve A), together with the variation of percentage decomposition, via all other paths, with pressure (curve B). The fact that curve B appears to become negative at low pressure is probably because the value of 9.1 found for k_{39}/k_{50} is too high. However, it can be seen that curve A shows only a small pressure dependence, indicating that the rate of formation of $CH_2F.CH_2F^*$ is approximately proportional to the pressure. Therefore, the assumption that $[CH_2F]^2/M$ is constant only causes a slight error in the determination of k_{39}/k_{50}.

Apart from the recombination of CH_2F radicals in reaction (38), the following reaction will take place:

$$CH_2F + H \longrightarrow CH_3F^* \qquad (12)$$

FIGURE 28.

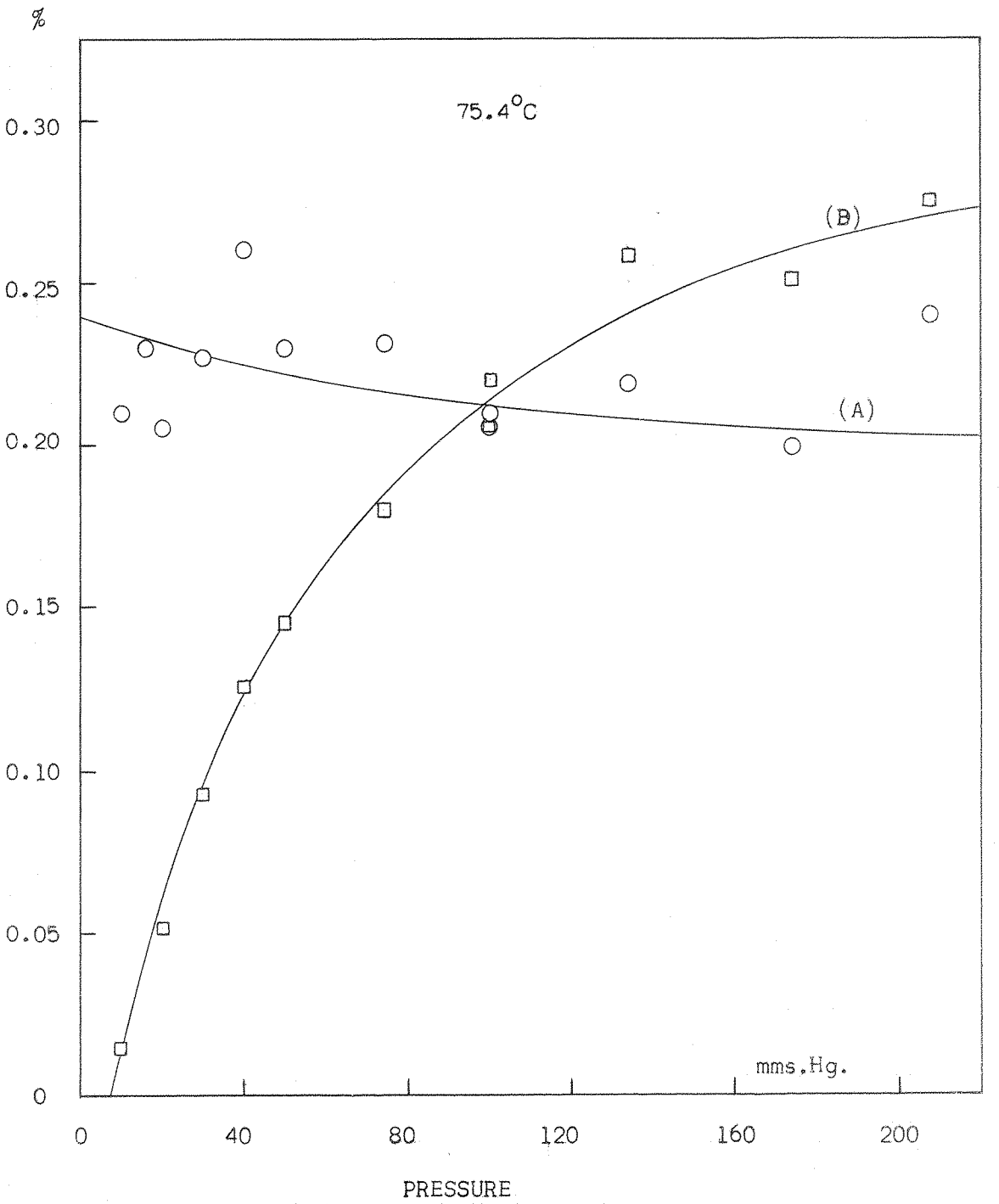

% Decomposition via Paths (A) and (B). (CH_3F)

Again it can be assumed that all activated molecules formed in reaction (12) will decompose before they can be deactivated by collision:

$$CH_3F^* \longrightarrow :CH_2 + HF \qquad (13)$$

The proportion of the total decomposition represented by curve B in Figure 28 will be mainly due to reaction (12). The sharp fall-off in this curve towards low pressure can be explained by assuming that hydrogen atoms are rapidly scavenged by olefins produced in hydrogen fluoride elimination reactions, thus reducing the rate of reaction (12).

The methylene produced in (13) can either dimerize, react with a hydrogen atom or insert into the C-H bond in methyl fluoride:

$$:CH_2 + :CH_2 \longrightarrow CH_2 = CH_2 \qquad (51)$$

$$:CH_2 + H \longrightarrow CH_3 \qquad (14)$$

$$:CH_2 + CH_3F \longrightarrow CH_3.CH_2F^{***} \qquad (48)$$

In the case of reaction (48), decomposition of methyl fluoride will occur which does not proceed via quenching of Hg^*, so that the total decompositon observed (Figure 26) will not all be the result of the quenching reaction (49). The product of insertion is very highly excited (about 115 kcal.mole^{-1} (27)) and over the pressure range studied can be considered to be incapable of collisional stabilization, i.e. only (33a) occurs:

$$CH_3CH_2F^{***} \longrightarrow CH_2 = CH_2 + HF. \qquad (33a)$$

The following simplified mechanism can be used to represent only those reactions involving the products of direct quenching:

Mechanism 1

$$Hg^* + CH_3F \xrightarrow{(49)} CH_2F + H + Hg$$

$$CH_2F + CH_2F \xrightarrow{(38)} CH_2F.CH_2F^* \xrightarrow{(39)} CH_2{=}CHF + HF$$

$$CH_2F.CH_2F^* \xrightarrow[M]{(50)} CH_2F.CH_2F$$

$$H + CH_2F \xrightarrow{(12a)} {}^1CH_2 + HF$$

$${}^1CH_2 + CH_3F \xrightarrow{(52)} CH_2 = CH_2 + HF$$

$$H + CH_2 = CHF \xrightarrow{(40)} CH_3.CHF$$

$$H + CH_2 = CH_2 \xrightarrow{(34)} C_2H_5 \ .$$

As this mechanism stands, the radicals produced in reactions (34) and (40) do not react with a further hydrogen atom. Applying a steady-state treatment to all the intemediates in mechanism 1, the following equations can be derived for the rates of formation of products via path A, reaction (38) and via path B, reaction (12):

$$R_{38} = k_{49}\left[Hg^*\right]\left[CH_3F\right]\left(\frac{1 + k_{50}\left[M\right]/k_{39}}{3 + 4k_{50}\left[M\right]/k_{39}}\right) \qquad (3)$$

$$R_{12} = k_{49}\left[Hg^*\right]\left[CH_3F\right]\left(\frac{1 + 2k_{50}\left[M\right]/k_{39}}{3 + 4k_{50}\left[M\right]/k_{39}}\right) \ . \qquad (4)$$

Both these equation express the rates of formation of products containing two carbon atoms and these rates are therefore equal to half the rate of decomposition of methyl fluoride by the

relative paths.

If the above mechanism I is modified by the inclusion of the following two reaction,

$$H + CH_3CHF \xrightarrow{(41)} CH_3CH_2F^*$$

$$H + C_2H_5 \xrightarrow{(53)} C_2H_6^*$$

(i.e. each olefin molecule produced adds two hydrogen atoms), the rate equations become; for mechanism II,

$$R_{38} = k_{49}[Hg^*][CH_3F] \cdot \left(\frac{1 + k_{50}[M]/k_{39}}{2 + 3k_{50}[M]/k_{39}} \right) \quad (5)$$

$$R_{12} = k_{49}[Hg^*][CH_3F] \cdot \left(\frac{k_{50}[M]/k_{39}}{2 + 3k_{50}[M]/k_{39}} \right) \quad (6)$$

(The derivation of equations(3) - (6) is given in Appendix II.) Substituting values of $k_{50}[M]/k_{39}$ into these equations gives the relative rates of decomposition via paths (A) and (B) shown in Table I :

TABLE I

	Pressure (mms.Hg)	Rate of Decompostion x $(k_{49}[Hg^*][CH_3F])^{-1}$	
		Path (A)	Path (B)
Mechanism I	0	0.67	0.67
	9.1	0.65	0.71
	91	0.57	0.86
	∞	0.50	1.00
Mechanism II	0	1.00	0
	9.1	0.95	0.09
	91	0.80	0.40
	∞	0.67	0.67

Comparing these values with the curves in Figure 28, it can be seen that neither mechanism gives a completely adequate description over the entire pressure range, but it should be remembered that both mechanisms are oversimplifications of the true state of affairs, which probably lies somewhere between these extremes. In addition, the ethyl fluoride molecule formed in reaction (41) of mechanism II will contain nearly 100 Kcal.mole^{-1} of excitation energy and hence will rapidly eliminate hydrogen fluoride to yield ethylene. Any

ethylene formed in this way will tend to decrease the hydrogen atom concentration still further. Reaction (53) also produces an excited molecule, which can dissociate to two methyl radicals. Hydrogen atoms can then be removed by the formation of methane:

$$CH_3 + H + M \longrightarrow CH_4 + M \qquad (15a)$$

Another reaction which should be considered is hydrogen abstraction from methyl fluoride by the hydrogen atoms:

$$H + CH_3F \longrightarrow CH_2F + H_2 \qquad (37)$$

Nevertheless, in spite of the inadequacy of both mechanisms, the sharp increase in curve (B) with pressure and the much smaller accompanying fall-off in curve (A) is predicted.

In view of the above discussion, it would now appear that the best measure of the percentage decomposition as a result of direct quenching of Hg* atoms is the value of the intercept at zero pressure in Figure 26, i.e. about 0.15%. This value can be used to determine an approximate rate constant for the chemical quenching of $Hg^*(^3P_1)$ atoms by methyl fluoride. In terms of the quenching mechanism given above, the rate of chemical quenching, R_{49}, is given by

$$R_{49} = \frac{k_b k_e \; I_{abs} \left[CH_3F\right]}{(k_{-b} + k_c + k_d + k_e)k_a} \quad , \qquad (7)$$

where $$\frac{k_b k_e}{(k_{-b} + k_c + k_d + k_e)} = k_{49} \quad .$$

The rate constant, k_a, for resonance phosphorescence in the present system is smaller than the corresponding rate constant, k_o, for an

isolated Hg* ($^3P_1$) atom, due to imprisonment of radiation. At the high mercury concentration used (1.2×10^{-3}mm. Hg.), light emitted from an excited mercury atom will be re-absorbed and re-emitted several times before escaping from the reaction vessel via the walls. Hence an imprisonment correction factor (c) must be applied, such that $k_a = ck_o$, where $c<1$ and is dependent on mercury vapour pressure, cell geometry and temperature, but not on the nature of the quencher (31). In this system the value of c can only be estimated and a value of 0.1 was chosen. Since $k_o = 9.1 \times 10^6$ sec^{-1}, k_a is about 1×10^6 sec^{-1}. The effective reaction volume was taken to be about 10 mls. Using these values and the light input rate of 2.0×10^{16} quanta.sec^{-1}, k_{49} can be calculated to be about $1 \times 10^{+5}$ l.mole^{-1}.sec^{-1}. This value is only accurate to an order of magnitude, but it significantly lower than the quenching rate constants reported for methane and fluoroform (1.1×10^9 and 5×10^7 l.mole^{-1} sec^{-1}) (32). However, both these reported values were obtained by the physical method (see Introduction), in which the measured quenching efficiency corresponds to both chemical quenching and quenching to the metastable state. Therefore, where quenching to the metastable state is important, the quenching rate constant estimated by the physical method will be larger than that from chemical data (34). It is, therefore, probable that the rate constant for chemical quenching alone for fluoroform (and also possibly methane) is significantly

lower than the value quoted above.

A model for the collision complex between Hg* ($^3P_1$) and a paraffin, RH, has been proposed [31] in which the mean lifetime of the complex is assumed to increase with increasing polarizability of RH and with increasing R-H bond strength. Since the C-H bond dissociation energy in fluoroform is high (106 kcal.mole^{-1})[6] and its polarizability larger than methane, k_c and k_d will be relatively more important. The role of metastable Hg' (^3P_o) (whose deactivation by ground state mercury atoms appears to be more important than chemical quenching processes)[35] in the quenching by fluoroform, and the other fluoromethanes, may therefore be of much greater importance than in the case where methane is the quencher.

The small drop in the quantum yield of decomposition products that was observed with an increase in temperature could now be explained in terms a drop in the hydrogen atom concentration (and hence the decompositon via path B) with increasing temperature, due to the faster rate of hydrogen atom addition to the olefins (E_A = 4 - 5 kcal.mole^{-1}). Another possible cause is a drop in the light intensity emitted from the lamp at the higher temperature. It has been shown [36] that the output of a low pressure mercury resonance lamp is very sensitive to the temperature of the lamp wall, especially at higher lamp currents. (The lamps used operated at about 120 mA.) Since the lamp was housed only in a metal tube

to protect it from drafts, and was situated close to the furnance window, it is possible that the change in furnace temperature caused a significant change in the ambient operating temperature of the lamp. The ambient temperature of the lamp was, however, not monitored, nor has the variation of lamp output with furnace temperature been studied.

It was shown above that a plot of $(\%\ CH_2FCH_2F)^{-1}$ against $(\text{pressure})^{-1}$ (Figure 27) was approximately linear and gave a value for k_{39}/k_{50} of 9.1 cm. A similar plot for $CH_3.CH_2F$ is shown in Figure 29 and can also be seen to be linear above 30 mm. Hg. Most ethyl fluoride will beformed by radical combinations

$$CH_3 + CH_2F \longrightarrow CH_3.CH_2F^{**} \qquad (42)$$

$$CH_3CH_2F^{**} \longrightarrow CH_2 = CH_2 + HF \qquad (33b)$$

$$CH_3.CH_2F^{**} + M \longrightarrow CH_3.CH_2F + M \qquad (54)$$

Hence the linearity of Figure 29 suggests that $[CH_3] \cdot [CH_2F] / [M]$ is approximately constant except at the lowest pressures. The slope-to-intercept ratio gives a value of about 38 cm. for k_{33b}/k_{54}. Values of this ratio have been reported in other systems; 14 cm. in the photolysis of a 1:1 mixture of acetone and 1,3 - difluoroacetone [27], and 25 cm. in the photolysis of monofluoroacetone [12], both at 75°C. Where monofluoroacetone was the quenching molecule, $(k_{33b}/k_{54})/(k_{39}/k_{50})$ was found to be about 4.2. The same value for this ratio was found in this system, where methyl fluoride is

FIGURE 29

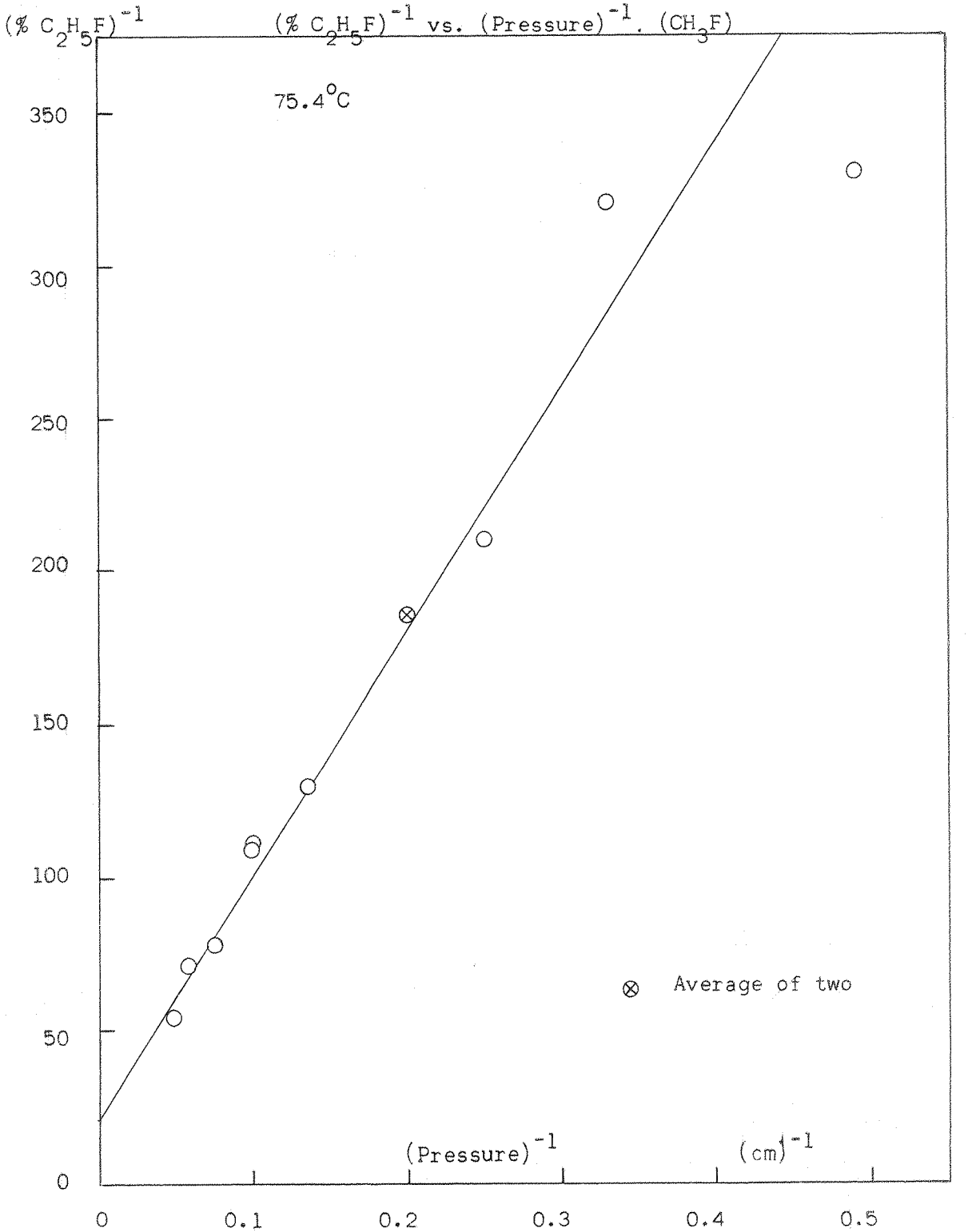
(% C_2H_5F)$^{-1}$
(% C_2H_5F)$^{-1}$ vs. (Pressure)$^{-1}$. (CH_3F)
75.4°C
350
300
250
200
150
100
50
0
⊗ Average of two
(Pressure)$^{-1}$
(cm)$^{-1}$
0
0.1
0.2
0.3
0.4
0.5

the quencher. In view of the indirect nature of the estimation of this ratio in this work and the large possible errors involved, the agreement is remarkably good.

Considering the following reactions only,

$$CH_3 + CH_3 \xrightarrow{(21)} C_2H_6$$

$$CH_3 + CH_2F \xrightarrow{(42)} C_2H_5F^{**} \xrightarrow[-HF]{(33b)} CH_2 = CH_2$$

$$C_2H_5F^{**} \xrightarrow[M]{(54)} C_2H_5F$$

$$CH_2F + CH_2F \xrightarrow{(38)} CH_2F.CH_2F^{*} \xrightarrow[-HF]{(39)} CH_2 = CHF$$

$$CH_2F.CH_2F^{*} \xrightarrow[M]{(50)} CH_2F.CH_2F$$

equation (8) can be derived, using a steady-state treatment for the activated molecules (see Appendix II), thus eliminating radical concentrations:

At constant time,

$$\frac{(\%\ C_2H_5F)^2}{(\%C_2H_6)(\%\ CH_2F.CH_2F)} = \frac{(k_{42}k_{54}/k_{33b})^2\,[M]\,(1 + k_{50}[M]/k_{39})}{k_{21}k_{38}k_{50}/k_{39}\,(1 + k_{54}[M]/k_{33b})^2} \qquad (8)$$

Using k_{39}/k_{50} = 9.1 cm. and k_{33b}/k_{54} = 38 cm., the left hand side of equation (8) was plotted against $[M]\,(1 + k_{50}[M]/k_{39})/(1 + k_{54}[M]/k_{33b})^2$, as shown in Figure 30. This plot should be a straight line, passing through the origin, and this is shown to be true if the points at the lowest three pressures are ignored. The slope of this line through the remaining points gives

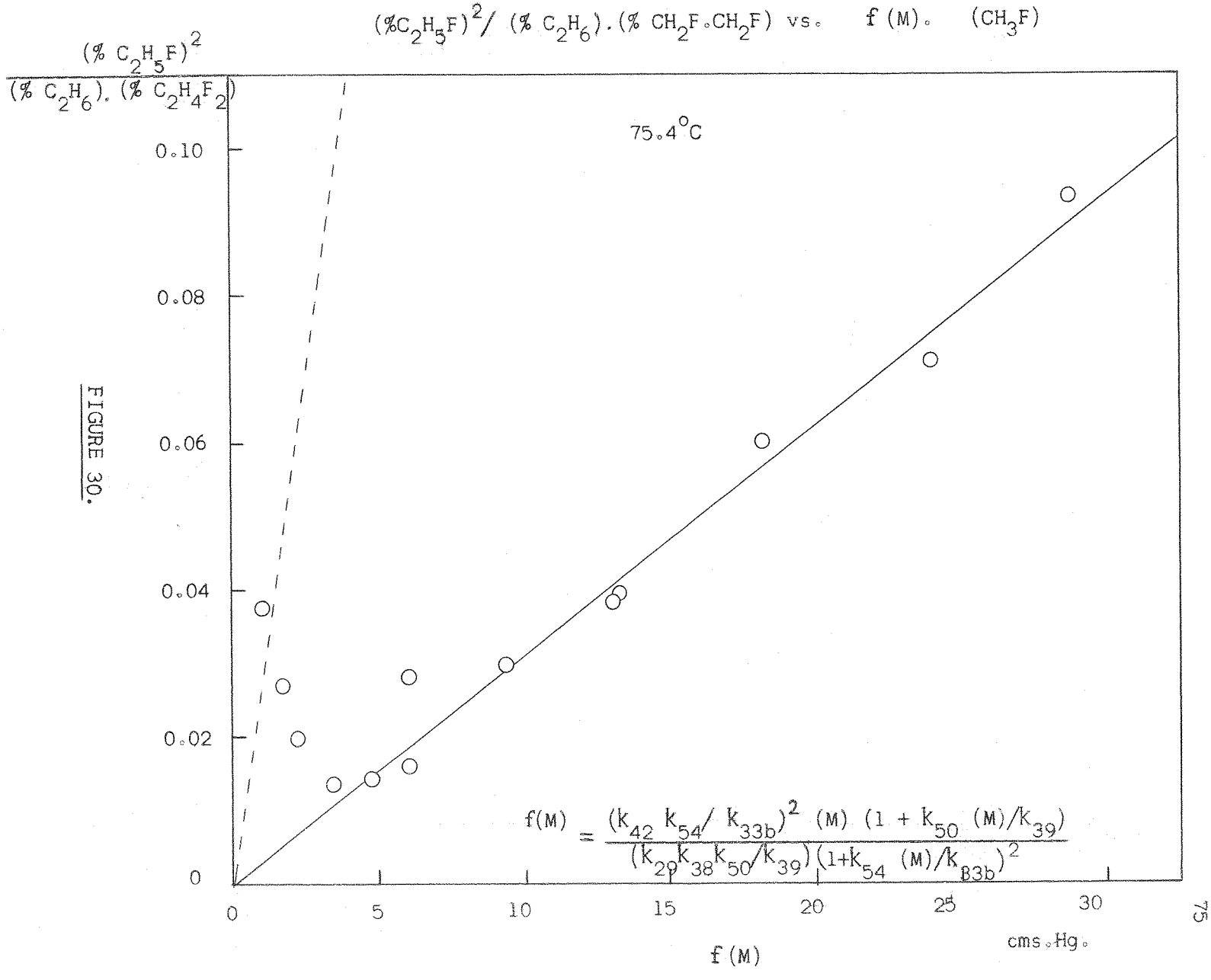
$(\%C_2H_5F)^2 / (\%\ C_2H_6).(\%\ CH_2F.CH_2F)$ vs. f (M). (CH_3F)
$\frac{(\%\ C_2H_5F)^2}{(\%\ C_2H_6).(\%\ C_2H_4F_2)}$
75.4°C
0.10
0.08
0.06
0.04
0.02
0
0
5
10
15
20
25
30
f (M)
cms. Hg.
$f(M) = \frac{(k_{42}\ k_{54}/\ k_{33b})^2\ (M)\ (1 + k_{50}\ (M)/k_{39})}{(k_{29}k_{38}k_{50}/k_{39})(1+k_{54}\ (M)/k_{83b})^2}$
75

FIGURE 30.

a value of 0.73 for the ratio $k_{42}/(k_{21}k_{38})^{\frac{1}{2}}$. Collision theory predicts a value of 2.1 for this ratio, using collision diameters $\sigma_{CH_3} = 3.5\text{Å}$ and $\sigma_{CH_2F} = 4.0\text{Å}$, and assuming that the reactions have identical activation energies and steric factors, usually taken as zero and unity, respectively. The large discrepancy between these two values is almost certainly due to the assumption in this treatment that all ethane is formed by reaction (21). It appears that the majority of ethane is formed via reaction (53),

$$C_2H_5 + H \longrightarrow C_2H_6^* \qquad (53)$$

$$C_2H_6^* + M \longrightarrow C_2H_6 + M \quad , \qquad (55)$$

except at low pressures were dissociation of the activated ethane is important:

$$C_2H_6^* \longrightarrow CH_3 + CH_3 \qquad (56)$$

Thus, at the lowest pressures the majority of ethane is formed by reaction (21) and the points approach the line predicted by collision theory, shown as a dotted line in Figure 30. Some justification for this explanation can be found in Figure 31, a plot of $(\%C_2H_6)^{-1}$ against $(\text{pressure})^{-1}$, which is approximately linear above 20 mm.Hg. This line yields a value of 1.8 cm. for k_{56}/k_{55}, assuming ethane is formed only via reaction (53) and $[C_2H_5].[H]/[M]$ is a constant. In a system where diethyl ketone was the deactivating molecule (M), k_{56}/k_{55} was found to be 0.35 cm. at 67°C [37], i.e. methyl fluoride appears to be about five times less efficient in quenching the

FIGURE 31

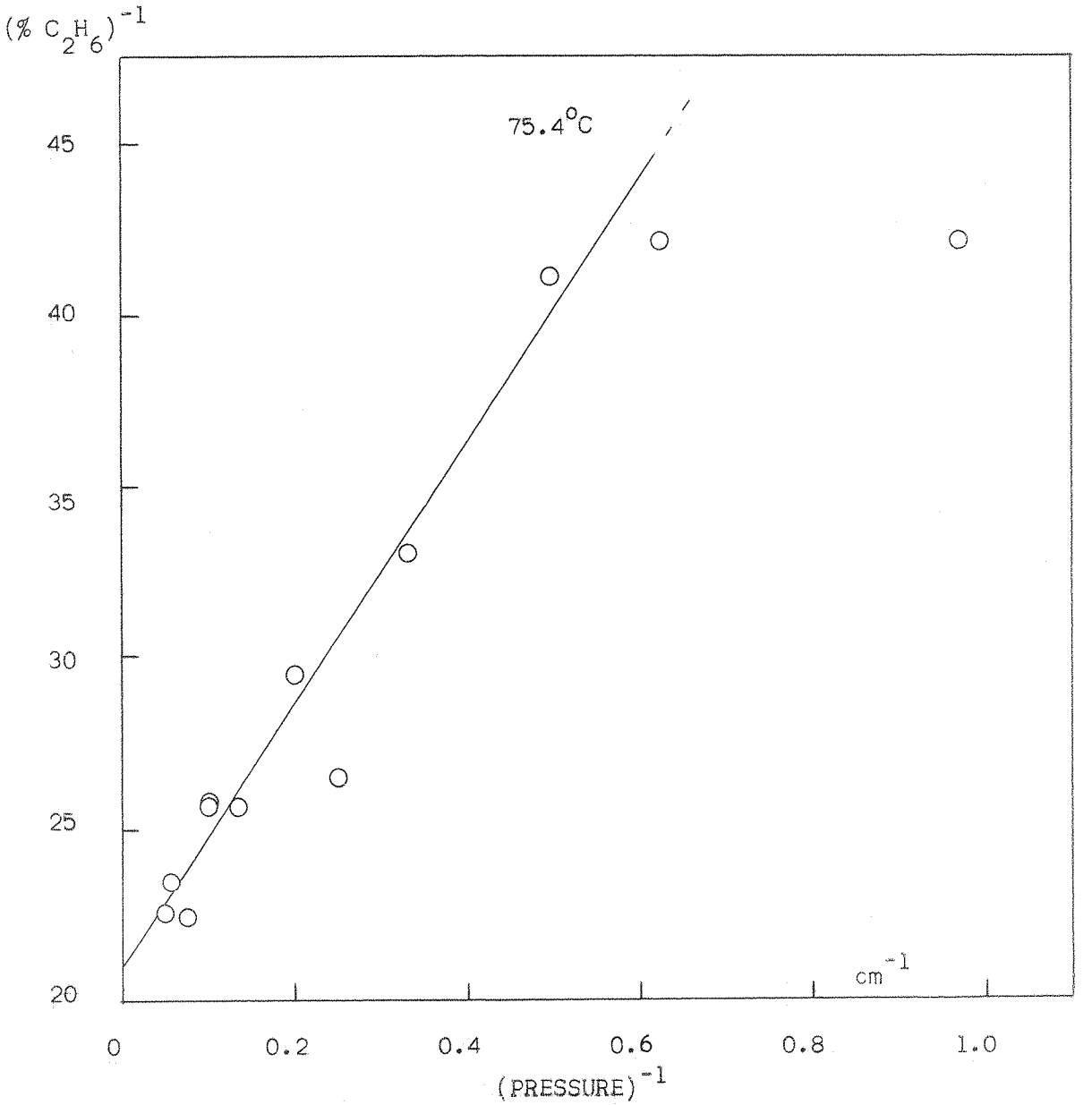

(% C_2H_6)$^{-1}$ vs. (Pressure)$^{-1}$. (CH_3F)

excited molecule than diethyl ketone. This seems to be reasonable in view of the fact that methyl fluoride was shown to be about four times less efficient as a quencher of "hot" molecules above than monofluoroacetone.

The following simplified mechanism is proposed to explain the formation of the observed products:

$$CH_3F + Hg^* \longrightarrow CH_2F + H + Hg \qquad (49)$$

$$H + H + M \longrightarrow H_2 + M \qquad (2)$$

$$CH_2F + H \longrightarrow :CH_2 + HF \qquad (12a)$$

$$2{:}CH_2 \longrightarrow CH_2 = CH_2 \qquad (51)$$

$$CH_3F + {:}CH_2 \longrightarrow CH_2 = CH_2 + HF \qquad (52)$$

$$:CH_2 + H \longrightarrow CH_3 \qquad (14)$$

$$2CH_3 \longrightarrow C_2H_6 \qquad (21)$$

$$CH_3 + H + M \longrightarrow CH_4 + M \qquad (15a)$$

$$2CH_2F \xrightarrow{(38)} CH_2F.CH_2F^* \begin{cases} \xrightarrow{(39)} CH_2 = CHF + HF \\ \xrightarrow[M]{(50)} CH_2F.CH_2F \end{cases}$$

$$CH_3 + CH_2F \xrightarrow{(42)} CH_3CH_2F^{**} \begin{cases} \xrightarrow{(33b)} CH_2 = CH_2 + HF \\ \xrightarrow[M]{(54)} CH_3CH_2F \end{cases}$$

$$CH_2 = CHF + H \longrightarrow CH_3CHF \quad (40)$$

$$CH_3CHF + H \longrightarrow CH_2 = CH_2 + HF \quad (41a)$$

$$CH_3CHF + CH_3 \longrightarrow \text{iso} - C_3H_7F^* \quad (44)$$

$$CH_3.CHF + CH_2F \longrightarrow CH_3CHF.CH_2F \quad (57)$$

$$CH_2 = CH_2 + H \longrightarrow C_2H_5 \quad (34)$$

$$C_2H_5 + H \xrightarrow{(52)} C_2H_6^* \begin{cases} \xrightarrow{(56)} 2CH_3 \\ \xrightarrow[M]{(55)} C_2H_6 \end{cases}$$

$$C_2H_5 + CH_3 \longrightarrow C_3H_8 \quad (35)$$

$$C_2H_5 + CH_2F \longrightarrow n\text{-}C_3H_7F^* \quad (43)$$

$$2C_2H_5 \longrightarrow n\text{-}C_4H_{10} \quad (36)$$

$$\text{iso} - C_3H_7F^* \text{ (or n} - C_3H_7F^*) \longrightarrow CH_3CH = CH_2 + HF \quad (45)$$

$$CH_3CH = CH_2 + H \longrightarrow CH_3CHCH_3 \quad (46)$$

$$CH_3.CHCH_3 + CH_3 \longrightarrow \text{iso} - C_4H_{10} \quad (47)$$

$$CH_3.CHCH_3 + CH_2F \longrightarrow \text{iso} - C_4H_9F \quad (58)$$

$$SiO_2 + 4HF \longrightarrow SiF_4 + 2H_2O$$

Although the products of reactions (57) and (58) were not identified, they were assumed to be the only two unidentified products observed. The activation energy for hydrogen fluoride

elimination from iso-propyl fluoride appears to be considerably lower than that for n-propyl fluoride[27], but owing to expected relative importance of reaction (43) compared to (44), both activated molecules probably produce a significant amount of propylene by reaction (45).

Although chemical quenching was only observed in the case of methyl fluoride, it must be stressed that there is no reason to suppose that it does not occur in the cases of difluoromethane and fluoroform. It should be remembered that, due to the expected smaller quenching efficiencies, detection of the resulting very low product yields by hot-wire detector would be very difficult, and the highly fluorinated products also have very low sensitivities with respect to the flame ionization detector.

e) Conclusion

It has been shown that when mixtures of hydrogen and fluoromethanes undergo mercury photosensitized decompositon, the product is almost exclusively methane. Only quenching of excited mercury atoms by hydrogen is important, and the temperature dependence of the rate of methane formation can be assumed to be due to the activation energy of hydrogen abstraction from the fluoromethane by hydrogen atoms, although much lower yields than were obtained in this work are desirable due to the competitive hydrogen abstraction from the product. Further work is required to confirm the occurrence of the

methylene intermediates proposed.

In the case of chemical quenching by methyl fluoride, the observed pressure dependence of the reaction rate can be explained in terms of methylene as an intermediate. Most products arise from the elimination of hydrogen fluoride from chemically activated molecules, but since olefins are rapidly consumed in this system, stabilization-to-elimination rate ratios can not be determined directly. Determination of quenching efficiencies by the nitrous oxide method and comparison with results from the physical method is required to show the importance of quenching to the metastable state by fluoromethanes. Chemical quenching by difluoromethane and fluoroform requires further careful study, although as in the case of methyl fluoride, the primary quenching process can be expected to involve a C-H bond scission.

* * *

APPENDIX I

B.pt. (°C)	Compound	Relative Retention Times at 75°C for:	
		Silica Gel Column	Alumina Column
-162	CH_4	0.32	0.575
-79	CH_3F	6.00	2.37
-52	CH_2F_2	5.47	3.67
-82	CHF_3	2.08	3.02
-128	CF_4	0.37	0.59
-88	C_2H_6	1.00	1.00
-25	$CH_3.CHF_2$	31.6	9.7
-47	$CH_3.CF_3$	8.65	3.65
≤ -20	$CHF_2.CHF_2$	> 17	22.8
-50	$CHF_2.CF_3$	7.89	9.6
-78	C_2F_6	1.09	1.00
-104	$CH_2 = CH_2$	1.61	1.22
-74	$CH_2 = CF_2$	2.23	1.52
-78	$CF_2 = CF_2$	1.50	1.14
-42	C_3H_8	3.5	1.67
0	$n\text{-}C_4H_{10}$	8.4	

B.pt. (°C)	Compound	Relative Retention time at 100°C for:	
		Silica Gel Column	PhasePak"Q" Column
-162	CH_4	0.365	0.251
-79	CH_3F	4.36	0.395
-104	C_2H_4	1.49	~0.39
-88	C_2H_6	1.00	0.525
-38	C_2H_5F		1.00
30	$CH_2F.CH_2F$		2.13
-84	C_2H_2	3.09	~0.4
-42	C_3H_8	2.90	1.34
-47	C_3H_6		1.23
-10	iso-C_3H_7F		2.52
-3	n-C_3H_7F		3.07
?	$CH_3.CHF.CH_2F$(?)		5.13
-51	$CH_2 = CHF$	3.66	0.574
-10	iso-C_4H_{10}		3.39
0	n-C_4H_{10}		4.27
16	iso-C_4H_9F(?)		7.95

Calibration Factors for F. I. D. (normal operation)

CH_4	0.207
CH_3F	1.00
CH_2F_2	0.431
CHF_3	0.265
C_2H_6	0.108
$CH_3.CF_3$	0.120

Calibration Factors for F. I. D. (outlet blocked)

Silica Gel (H_2, 4p.s.i.; Air, 16 p.s.i.)

CH_4	0.753
C_2H_4	0.368
C_2H_6	0.400
CH_3F	1.00
C_3H_8	0.256

PhasePak"Q" (H_2, 5p.s.i.; Air, 16psi)

CH_4	0.90	
CH_3F	1.00	
C_2H_6	0.457	
C_3H_8	0.284	
C_2H_5F	0.416	
$CH_2F.CH_2F$	0.460	
C_3H_7F	0.310	
C_4H_{10}	0.208	
$CH_3CHF.CH_2F$	0.35	(Estimated)
iso-C_4H_9F	0.23	(Estimated)

APPENDIX II

(i) Derivation of Equations (3) - (6)

Considering the following reactions only:

Mechanism I. $Hg^* + CH_3F \xrightarrow{(49)} CH_2F + H + Hg$

$$2CH_2F \xrightarrow{(38)} CH_2F.CH_2F^* \begin{cases} \xrightarrow{(39)} CH_2 = CHF + HF \\ \xrightarrow[(50)]{M} CH_2F.CH_2F \end{cases}$$

$$H + CH_2F \xrightarrow{(12)} :CH_2 + HF$$

$$CH_2 + CH_3F \xrightarrow{(52)} CH_2 = CH_2 + HF$$

$$H + CH_2{=}CHF \xrightarrow{(40)} CH_3.CHF$$

$$H + CH_2{=}CH_2 \xrightarrow{(34)} C_2H_5$$

the following stationary-state expression can be written:

For $[H]$,

$$k_{49}[Hg^*].[CH_3F] = k_{12}[CH_2F][H] + k_{40}[CH_2{=}CHF][H] + k_{34}[CH_3{=}CH_2][H].$$

For $[CH_2F]$,

$$k_{49}[Hg^*][CH_3F] = 2k_{38}[CH_2F]^2 + k_{12}[CH_2F][H]$$

For $[CH_2{=}CH_2]$,

$$k_{34}[CH_2{=}CH_2][H] = k_{52}[CH_2][CH_3F] = k_{12}[CH_2F][H]$$

For $[CH_2{=}CHF]$,

$$k_{40}[CH_2{=}CHF][H] = k_{39}k_{38}[CH_2F]^2/(k_{39} + k_{50}[M]).$$

$$\therefore [H] = \frac{k_{49}[Hg^*][CH_3F]}{\frac{k_{39}k_{38}[CH_2F]^2}{(k_{39} + k_{50}[M])[H]} + 2k_{12}[CH_2F]}$$

$$[H] = \frac{k_{49}[Hg^*][CH_3F]}{\frac{k_{49}[Hg^*][CH_3F] - k_{12}[CH_2F][H]}{2(k_{39} + k_{50}[M])[H]} + 2k_{12}[CH_2F]}$$

$$\therefore k_{12}[CH_2F][H] = \frac{k_{49}[Hg^*][CH_3F].\left(1 - \frac{k_{39}}{2(k_{39} + k_{50}[M])}\right)}{2 - \frac{k_{39}}{2(k_{39} + k_{50}[M])}}$$

$$\therefore R_{12} = k_{12}[CH_2F][H]$$

$$= k_{49}[Hg^*][CH_3F].\frac{1 + 2k_{50}[M]/k_{39}}{3 + 4k_{50}[M]/k_{39}} \quad \text{..... Equation (4)}$$

$$\therefore R_{38} = k_{38}[CH_2F]^2$$

$$= \frac{k_{49}[Hg^*][CH_3F]}{2}.\left(1 - \frac{1 + 2k_{50}[M]/k_{39}}{3 + 4k_{50}[M]/k_{39}}\right)$$

$$= k_{49}[Hg^*][CH_3F].\frac{1 + k_{50}[M]/k_{39}}{3 + 4k_{50}[M]/k_{39}} \quad \text{..... Equation (3)}$$

Mechanism II.

If reaction (40) is followed by

$CH_3CHF + H \xrightarrow{(41)} CH_3CH_2F^*$,

and reaction (34) is followed by

$$C_2H_5 + H \xrightarrow{(53)} C_2H_6^*,$$

only the equation for the steady state in [H] is changed, i.e.,

$$k_{49}[Hg^*][CH_3F] = k_{12}[CH_2F][H] + 2k_{40}[CH_2{=}CHF][H] + 2k_{34}[CH_2{=}CH_2][H]$$

$$\therefore k_{12}[CH_2F][H] = \frac{k_{49}[Hg^*][CH_3F].\left(1 - \frac{k_{39}}{k_{39} + k_{50}[M]}\right)}{3 - \frac{k_{39}}{k_{39} + k_{50}[M]}}$$

$$\therefore R_{12} = k_{49}[Hg^*][CH_3F].\frac{k_{50}[M]/k_{39}}{2 + 3\,k_{50}[M]/k_{39}} \quad \text{.....Equation (6)}$$

$$\text{and } R_{38} = k_{49}[Hg^*][CH_3F].\frac{1 + k_{50}[M]/k_{39}}{2 + 3k_{50}[M]/k_{39}} \quad \text{.....Equation (5)}$$

(ii) Derivation of Equation (8)

Considering the following reactions:

$$CH_3 + CH_3 \xrightarrow{(21)} C_2H_6$$

$$CH_3 + CH_2F \xrightarrow{(42)} C_2H_5F^{**} \begin{cases} \xrightarrow{(33b)} CH_2 = CH_2 + HF \\ \xrightarrow[M]{(54)} C_2H_5F \end{cases}$$

$$CH_2F + CH_2F \xrightarrow{(38)} CH_2F.CH_2F^* \begin{cases} \xrightarrow{(39)} CH_2 = CHF + HF \\ \xrightarrow[M]{(50)} CH_2F.CH_2F \end{cases},$$

$$R_{21} = k_{21}[CH_3]^2$$

$$R_{42} = k_{42}[CH_3][CH_2F].\frac{k_{54}[M]}{k_{33b} + k_{54}[M]}$$

$$R_{38} = k_{38}\left[CH_2F\right]^2 \cdot \frac{k_{50}\left[M\right]}{k_{39} + k_{50}\left[M\right]}$$

At constant time, $\dfrac{(\%\ C_2H_5F)^2}{(\%C_2H_6)(\%CH_2F.CH_2F)} = \dfrac{(R_{42})^2}{(R_{21})(R_{38})}$

$$= \frac{(k_{42}k_{54})^2\left[M\right]^2 \cdot (k_{39} + k_{50}\left[M\right])}{(k_{33b} + k_{54}\left[M\right])^2 \cdot k_{21}k_{38}k_{50}\left[M\right]}$$

$$\therefore \frac{(\%C_2H_5F)^2}{(\%C_2H_6)(\%CH_2F.CH_2F)} = \frac{(k_{42}k_{54}/k_{33b})^2\left[M\right](1 + k_{50}\left[M\right]/k_{39})}{(k_{21}k_{38}k_{50}/k_{39})(1 + k_{54}\left[M\right]/k_{33b})^2} \quad \text{Eq. (8)}$$

REFERENCES.

(1)	R. A. Sieger and J. G. Calvert	J. Amer.Chem.Soc. 76, 5197 (1954).
(2)	R. E. Dodd and J. W. Smith	Research 8, 63 (1955).
(3)	P. B. Ayscough, J. C. Polanyi and E. W. R. Steacie	Canad. J. Chem. 33, 743 (1955).
(4)	P. B. Ayscough and E. W. R. Steacie	(a) Proc.Roy.Soc.A 234,476 (1956). (b) Canad. J. Chem. 34, 103 (1956). (c) J. Chem. Phys. 24, 944 (1956).
(5)	G. O. Pritchard, H. O. Pritchard, H. I. Schiff, and A. F. Trotman-Dickenson	Trans. Farad. Soc. 52, 849 (1956).
(6)	J. W. Coomber and E. Whittle	Trans. Farad. Soc. 62, 2183 (1966).
(7)	J. W. Coomber and E. Whittle	Trans Farad. Soc. 63, 1394 (1967).
(8)	Estimated from H_f^o calculated by H. J. Bernstein	J. Phys Chem. 69, 1550 (1965).
(9)	J. R. Dacey and J. W. Hodgins	Canad. J. Research, 28, 173 (1950).
(10)	G. O. Pritchard, M. Venugopalan, and T. F. Graham	J. Phys. Chem. 68, 1786 (1964).
(11)	R. D. Giles and E. Whittle	Trans. Farad. Soc. 61, 1425 (1965).
(12)	G. O. Pritchard and R. L. Thommarson	J. Phys. Chem. 71, 1674 (1967).
(13)	S. W. Benson and G. Haugen	J. Phys. Chem. 69, 3898 (1965).
(14)	G. O. Pritchard and J. T. Bryant	J. Phys. Chem. 70, 1441 (1966).
(15)	R. J. Cvetanovic, W. E. Falconer, and K. R. Jennings	J. Chem. Phys. 35, 1225 (1961).

(16) W. F. Edgell and L. Parts — J. Amer. Chem. Soc. 77, 4899 (1955).

(17) E. A. Jones, J. S. Kirby-Smith, P. J. H. Woltz and A. H. Nielson — J. Chem. Phys. 19, 242. (1951).

(18) E. Tschuikow-Roux
See also A. P. Modica and J. E. LaGraff — J. Chem. Phys. 42, 3639 (1965).
J. Chem. Phys. 44, 3375 (1966).

(19) (a) W. Mahler — Inorg. Chem. 2, 230 (1963).
(b) R. A. Mitsch — J. Amer. Chem. Soc. 87, 758 (1965).
(c) J. P. Simons — Nature 205, 1308 (1965).
(d) W. Fielding and H. O. Pritchard — J. Phys. Chem. 64, 278 (1960).
(e) I. P. Fisher, J. B. Homer and F. P. Lossing — J. Amer. Chem. Soc. 87, 957 (1965).

(20) J. M. Birchall, G. W. Cross and R. N. Haszeldine — Proc. Chem. Soc. 1960, 81.

(21) N. Cohen and J. Heicklen — J. Chem. Phys. 43, 871 (1965).

(22) R. A. Odum and R. Wolfgang — J. Amer. Chem. Soc. 85, 1050 (1963).

(23) D. W. Placzek, B. S. Rabinovitch, G. Z. Whitter and E. Tschuikow - Roux — J. Chem. Phys. 43, 4071 (1965).

(24) J. A. Bell and G. B. Kistiakowsky — J. Amer. Chem. Soc. 84, 3417 (1962).

(25) G. O. Pritchard and J. T. Bryant — J. Phys. Chem. 69, 1085 (1965).

(26) J. C. Amphlet and E. Whittle — Trans. Farad. Soc. 63, 2695 (1967).

(27) J. A. Kerr, A. W. Kirk, B. V. O'Grady, D. C. Phillips and A. F. Trotman-Dickenson — Farad. Soc. Disc. "Molecular Dynamics of Chemical Reactions of Gases", Univ. of Toronto, Sept. 1967.

(28) M. G. Bellas, O. P. Strausz and H. E. Gunning, — Canad. J. Chem. 43, 1022 (1965).

(29)	C. A. Heller	J. Chem. Phys. 28, 1255 (1958).
(30)	S. Penzes, O. P. Strausz and H. E. Gunning	J. Phys. Chem. 45, 2322 (1966).
(31)	K. Yang	J. Amer. Chem. Soc. 89, 5344 (1967).
(32)	R. J. Cvetanovic in Prog. Reaction Kinetics	Vol. 2, 39 (1964). Ed. G. Porter.
(33)	K. Yang	J. Amer. Chem. Soc. 86, 3941 (1964).
(34)	S. Penzes, A. J. Yarwood, O. P. Strausz and H. E. Gunning	J. Chem. Phys. 43, 4524 (1965).
(35)	J. E. McAlduff and D. J. Leroy	Canad. J. Chem. 43, 2279 (1965).
(36)	L. J. Heidt and H. B. Boyles	J. Amer. Chem. Soc. 73, 5723 (1951).
(37)	C. A. Heller and A. S. Gordon	J. Chem. Phys. 36, 2648 (1962).